Biophysical Reviews (2023) 15:447–473
https://doi.org/10.1007/s12551-023-01100-6

LETTER TO THE EDITOR

Bacterial toxins and heart function: heat-labile *Escherichia coli* enterotoxin B promotes changes in cardiac function with possible relevance for sudden cardiac death

Gonzalo Ferreira[1] · Romina Cardozo[1] · Santiago Sastre[2] · Carlos Costa[1] · Axel Santander[1] · Luisina Chavarría[1] · Valentina Guizzo[1] · José Puglisi[3] · G. L. Nicolson[4]

Received: 22 March 2023 / Accepted: 11 July 2023 / Published online: 22 July 2023

Abstract

Bacterial toxins can cause cardiomyopathy, though it is not its most common cause. Some bacterial toxins can form pores in the membrane of cardiomyocytes, while others can bind to membrane receptors. Enterotoxigenic *E. coli* can secrete enterotoxins, including heat-resistant (ST) or labile (LT) enterotoxins. LT is an AB_5-type toxin that can bind to specific cell receptors and disrupt essential host functions, causing several common conditions, such as certain diarrhea. The pentameric B subunit of LT, without A subunit (LTB), binds specifically to certain plasma membrane ganglioside receptors, found in lipid rafts of cardiomyocytes. Isolated guinea pig hearts and cardiomyocytes were exposed to different concentrations of purified LTB. In isolated hearts, mechanical and electrical alternans and an increment of heart rate variability, with an IC50 of ~0.2 µg/ml LTB, were observed. In isolated cardiomyocytes, LTB promoted significant decreases in the amplitude and the duration of action potentials. Na^+ currents were inhibited whereas L-type Ca^{2+} currents were augmented at their peak and their fast inactivation was promoted. Delayed rectifier K^+ currents decreased. Measurements of basal Ca^{2+} or Ca^{2+} release events in cells exposed to LTB suggest that LTB impairs Ca^{2+} homeostasis. Impaired calcium homeostasis is linked to sudden cardiac death. The results are consistent with the recent view that the B subunit is not merely a carrier of the A subunit, having a role explaining sudden cardiac death in children (SIDS) infected with enterotoxigenic *E. coli*, explaining several epidemiological findings that establish a strong relationship between SIDS and ETEC *E. coli*.

Introduction

There are several bacterial toxins that can potentially cause cardiomyopathy, which is a disease affecting the heart muscle (L'Heureux et al. 2020). However, it is important to note that bacterial toxins causing cardiomyopathy are relatively rare compared to other causes such as genetic factors, viral infections, or certain medications (Blauwet and Cooper 2010). Some examples of bacterial toxins associated with cardiomyopathy are those from *Corynebacterium diphtheriae*, *Streptococcus (Group A)*, *Staphylococcus dureus*, *Bacillus dnthracis*, and *Vibrio cholerae* (Huang and Wong 1989; Miller et al. 1987; Monticelli et al. 2018). The later one is linked to diarrhea and the gut, and it also shares a tight structural association with some toxins from *Escherichia coli* (*E. coli*), which is the main topic of this letter.

Escherichia coli is one of the most frequent and versatile Gram-negative classes of bacteria in the Earth's biosphere. It is also one of the most important bacteria in the normal intestinal flora of multicellular organisms, especially

✉ Gonzalo Ferreira
ferreira@fmed.edu.uy

1 Ion Channels, Biological Membranes and Cell Signaling Laboratory, Dept. Of Biophysics, Facultad de Medicina, Universidad de la Republica, Gral Flores 2125, 11800 Montevideo, CP, Uruguay

2 Ion Channels, Biological Membranes and Cell Signaling Laboratory, Dept. Of Biophysics and Centro de Investigaciones Biomédicas (CeInBio), Facultad de Medicina, Universidad de la Republica, Gral Flores 2125, 11800 Montevideo, CP, Uruguay

3 College of Medicine, California North State University, 9700 West Taron Drive, Elk Grove, CA 95757, USA

4 Institute for Molecular Medicine, Beach, Huntington, CA, USA

mammals. In general, it has a symbiotic commensal relationship with the organism in which it inhabits, but certain strains in humans and other mammals can also be deadly pathogens. For example, there are at least 6 strains of *E. coli* that can produce toxins that contribute to intestinal and extra-intestinal diseases (Kaper et al. 2004).

The enterotoxigenic (ETEC) strains are among the most common pathogenic strains of *E. coli* (Fleckenstein and Kuhlmann 2019). These strains are one of the main causes of diarrhea in children in the developing world and traveler's diarrhea in adults. These ETEC strains have also been linked to some forms of septic shock and sudden cardiac death in infants (Morris et al. 2009). The ETEC strains of *E. coli* produce different types of toxins, which are basically either heat-resistant (ST) or heat-labile (LT). The ST and LT enterotoxins target specific cell surface receptors that activate different intracellular pathways to alter cellular physiology (Dubreuil et al. 2016). For example, LT enterotoxins are usually composed of one A subunit and a pentamer of B subunits that assemble to form an AB_5 toxin structure (Beddoe et al. 2010; Fan et al. 2000). The AB_5 toxins are important pathogenic factors produced by many bacteria, including *Bordetella pertussis*, *Shigella dysenteriae*, *Vibrio cholerae*, and no less than two strains of *E. coli* (Beddoe et al. 2010; Gill and Richardson 1980; Spangler 1992). The AB_5 are also used as tools for studying cell signaling and physiology as well as potential drugs for the treatment of certain cancers and allergies (Beddoe et al. 2010). The heat-labile enterotoxin from *E. coli* is a member of the AB_5 toxin family, which comprises a single A subunit and five B subunits with high resemblance to the B subunit of the cholera toxin (Sixma et al. 1993).

The A subunit of the AB_5 enterotoxins has been identified as the main factor behind important changes in cells by altering the intracellular levels of cAMP through G-protein-coupled receptors promoting diarrhea [4]. Thus, the A subunit can stimulate G-proteins, thereby increasing intracellular concentrations of cAMP, which in turn can activate the CFTR chloride channel, leading to changes in water secretion (Thiagarajah and Verkman 2005). This mechanism was originally described for the homologous toxin produced by *V. cholera*, which can cause severe diarrhea.

The B subunit toxin, which is usually formed into a pentamer, was regarded previously as mostly a carrier for the delivery of the A or catalytic toxin subunit into target cells. Evidence has shown that the B toxin subunit binds specifically to ganglioside receptors (Supp. Fig. 1, PDB ID 3CHB) (Merritt et al. 1998; Mudrak and Kuehn 2010), and upon binding initiates subsequent cellular changes in target cells. It is known that *Cholera* and *E. coli* enterotoxins are highly homologous structurally, functionally, and immunologically (Dallas and Falkow 1980). Cholera enterotoxin can increase cardiac arrhythmias and ventricular fibrillation, thereby promoting sudden cardiac death (Huang and Wong 1989). By its specific binding and subsequent activity in target cells, the B toxin is also a virulence factor of the ETEC *E. coli* strains and can produce systemic pathogenic symptoms (Duan et al. 2019; Patry et al. 2019). Since the heat-labile-B-pentamer plays a role in ETEC pathogenesis, recent efforts have been made to inhibit its action (Xu et al. 2020; Zhu et al. 2017).

The B fraction or LTB toxins target specialized gangliosides and glycosphingolipids composed of ceramide, and oligosaccharides containing sialic acid. These specialized gangliosides can accumulate in cholesterol/glycosphingolipid-enriched membrane domains, also described as lipid rafts or glycosynaptic domains, which constitute extracellular receptor platforms for important signal transduction pathways (Mahfoud et al. 2010; Smith et al. 2004).

Common gangliosides, such as GM1, contain one sialic acid moiety (monosialotetrahexosylganglioside (Lloyd and Furukawa 1998)) and are involved in many important physiological events, such as signal transduction, cell adhesion, motility, and other functions (Zeller and Marchase 1992). It has been established that toxins containing B subunits bind specifically to GM1 receptors on many cell types and are also commonly found in lipid rafts (Dawson 2005; Fishman et al. 1993). The IC50 reported for B-subunit toxin binding to GM1 in vitro and in vivo are both close to 0.15 µg/ml (Hedges and Hardy 1996). Upon binding of the B-toxin to its cell surface receptor, a series of changes occur in these cells (Mudrak and Kuehn 2010). Several bacterial toxins act by initially binding to GM1 (Smith et al. 2004). Ganglioside localization in lipid rafts is also important in calcium (Ca^{2+}) signaling and modifying intracellular Ca^{2+} concentrations in several cell types (Pani and Singh 2009; Simons and Toomre 2000).

The binding of cholera B-toxin subunit to GM1 in sensory neurons and cultured cerebellar granule neurons has been reported to increase intracellular Ca^{2+} levels by approximately 10-fold (Milani et al. 1992; Wu et al. 1996). Similar results were obtained in rat lymphocytes, astrocytes, Jurkat cells, and 3T3 fibroblasts (Dixon et al. 1987; Gabellini et al. 1991; Spiegel and Panagiotopoulos 1988). These effects have been described as toxin-induced Ca^{2+} oscillations (Soderblom et al. 2002). Some Ca^{2+} effects occur in the absence of toxin-ganglioside binding, and even changes in ganglioside amounts by themselves have been shown to alter basal intracellular Ca^{2+} concentrations in pC12 cells (Hilbush and Levine 1992). Gangliosides regulate tyrosine kinases (PTK) (Julien et al. 2013). PTK, in turn, can modulate Ca^{2+} release in many cells by mechanisms that are not well understood (Mergler et al. 2003).

Gangliosides have been found to be important in several tissues, such as in the development, maturation, and maintenance of the myelin covering nerves in the nervous system

(Bremer et al. 1984; Posse de Chaves and Sipione 2010; Schnaar 2010). In the heart, gangliosides have a critical role in maintaining heart function, and this has been demonstrated in many types of metabolic cardiomyopathies (Guertl et al. 2000). Certain diseases, such as GM1 gangliosidosis type 1, can be caused by a deficiency in beta-galactosidase that results in reduced amounts of GM1. Alternatively, plasma and intracellular membranes can be altered in cells due to ganglioside accumulation, such as in cells of the nervous and cardiovascular systems, leading to an accumulation of ganglioside-containing intracellular vacuoles. In this case, the normal levels of GM1 are augmented, and as a result, there is a reduction in cardiac contractibility, followed by cardiac failure. However, this can be partially compensated for by dilatation and hypertrophy (Guertl et al. 2000).

The presence of ganglioside-enriched lipid rafts and sialic acid content play critical roles in determining intracellular Ca^{2+} levels (Marengo et al. 1998). Normal cardiac function requires specific controls on intracellular Ca^{2+} dynamics (Wang et al. 2004). Patterns of heartbeat waveforms, heart excitability, and tension levels have been related to intracellular Ca^{2+} concentrations, and these are collectively important factors that can determine if arrhythmias occur and can eventually give rise to sudden cardiac arrest (Laurita and Rosenbaum 2008).

In this letter, we examine the current knowledge of bacterial toxin effects in the heart focusing on the effects of LTB from *E. coli* in the heart. For the later, given the absence of data, we show original research using purified LTB toxin from *E. coli*. The effects were tested by applying extracellularly LTB to isolated guinea pig hearts and cultured heart cells. We monitored heart functioning upon extracellular binding of LTB to isolated guinea pig hearts as well as to isolated guinea pig cardiomyocytes. We found that LTB binding to GM1 causes modulation of heart and heart-cell functions, and we generated dose-response curves for some of these responses. At LTB concentrations near the IC50 binding to GM1 (0.13 to 0.18 µg/ml) (Spangler 1992), an alternans pattern of contraction was observed in isolated hearts, while in isolated cardiac myocytes, changes in action potential (AP) duration, ionic currents, and intracellular Ca^{2+} imaging were observed. The results suggest that (i) LTB binding to ganglioside in lipid rafts is an important modulator of intracellular Ca^{2} concentrations in cardiac myocytes, (ii) LTB binding to gangliosides can promote cardiac dysfunction in isolated hearts, and (iii) LTB binding disturbs Ca^{2+} homeostasis significantly, explaining the alternans pattern observed. It is known that impaired Ca^{2+} homeostasis leads to sudden cardiac death (Tzimas et al. 2017). This may contribute to explaining the implication of pathogenic *E. coli* in sudden cardiac infant deaths (Bettelheim et al. 1990; Blackwell et al. 2002). These results are consistent with the recent view that the B subunit is not merely a carrier of the A subunit, having an important role in the pathogenesis of *E. coli* (Duan et al. 2019).

Bacterial toxins and heart function

There are several ways in which bacterial toxins may impact heart function at the cellular level. Toxins may have different targets in most compartments of eukaryotic cells and a rough division can be made according to this (Masignani et al. 2006). The three main categories are as follows:

A) Those that act on the cell membrane of eukaryotic cells either through binding to receptors or forming pores. Both types can regulate indirectly or directly membrane permeability. In this letter, we will discuss this type and particularly the ones that exert their effect indirectly.
B) Those with an intracellular target that have to cross the cell membrane.
C) Those that have an intracellular target and are directly delivered by the bacteria into eukaryotic cells (Masignani et al. 2006).

As we have mentioned, one of them is through toxins that form a pore in the membrane such as streptolysin O (SLO), produced by group A *Streptococcus* such as *Streptococcus pyogenes*, in toxic shock syndromes (Bolz et al. 2015), or pneumolysin (PLY) produced by *Streptococcus pneumoniae* (Wang et al. 2017). Both toxins can be inserted into the membrane leading to a marked influx of Ca^{2+} through their pores yielding hypercontractility and pacing anomalies, producing dysfunctional cardiomyocytes and cardiomyopathy in the heart (Bolz et al. 2015). In zebrafish, *Clostridium difficile* toxin B produced cardiovascular damage with a reduction in blood flow and heart rate (Hamm et al. 2006). The action seems to involve caspase 3 (Hamm et al. 2006). Bacterial exotoxins from uncommon pathogens such as *Corynebacterium dyphteriae* and *Bacillus anthracis* can produce cardiomyopathy affecting cardiomyocytes. Myocarditis is a toxin complication that happens 1 week after the respiratory illness in diphtheria (Singh et al. 2020). The heparin-binding (EGF-like) growth factor is the blood receptor for the toxin, which in turn undergoes endocytosis and binds to specific membrane receptors changing expression patterns (Iwamoto et al. 1994). *Bacillus anthracis* produces the lethal toxin (LT), that induces cardiac dysfunction by mechanisms not well understood (Suffredini et al. 2015). Finally, *Staphylococcus aureus*, a bacterium commonly found on the skin and nasal passages, can produce pore-forming toxins like the α-toxin, that can damage the heart muscle (Grandel et al. 2009). These toxins can lead to toxic shock syndrome, a severe condition that can result in cardiac dysfunction and cardiomyopathy in some cases (Silversides et al. 2010).

Several bacterial toxins from the gut can have a direct impact on the function of the heart (Olson et al. 1989; Robert et al. 2012). *E. coli* strains, such as 0157:H7, have been reported to produce gastroenteritis and toxins that could be implicated in cardiovascular disease (Hizo-Abes et al. 2013). The gut microbiota has been recently found to be implicated in various cardiovascular disorders (Rahman et al. 2022; Witkowski et al. 2020), and toxins from the gut microbiota have been tightly associated with cardiovascular disease, particularly pro-inflammatory lipopolysaccharides, derived from Gram-negative bacteria, and trimethylamine N-oxide (Yamashita et al. 2021). Sudden cardiac death has been also reported in pediatric patients with *E. coli*-producing *Shiga*-like toxin (STEC) (Yesilbas et al. 2020). Some of those toxins may impact the intestine promoting diarrhea primarily, because they promote changes in membrane transport, either by a direct or indirect impact (Laohachai et al. 2003). Some of those bacteria are *Vibrio cholerae* and *E. coli*. Cholera toxins are similar to the ETEC *E. coli* toxins (Spangler 1992). The crystal structure of the cholera toxin B-pentamer bound to the receptor GM1 has been obtained (Merritt et al. 1994). It has been found in the hearts from isolated rats, that *Cholera* enterotoxin promotes arrhythmias in the presence of ischemia (Huang and Wong 1989). However, this has not been tested with the LTB fraction from ETEC *E. coli*, so far. We suppose that given the similarity between the toxins, an impact of LTB in the heart might be found. It is known that the B-subunit of ETEC *E. coli* binds with specificity and an affinity with an IC-50 of ~ 0.2 or 0.18 µg/ml to the GM1 receptor of cardiac cells (Minke et al. 1999), similarly to what it has been described for the cholera toxina B-pentamer.

Acute exposure of guinea-pig isolated hearts to LTB enterotoxin from *E. coli* promotes electrical and mechanical alternans

To test if LTB promotes any changes in cardiac function, we isolated hearts from guinea pigs following approved ethical procedures (approval protocol number 071140-000467-09, CHEA) to further applied the toxin. Isolated hearts were maintained at 37 °C with perfusion of Tyrode 1.8 Ca^{2+} solution with oxygen at a flow rate between 14 and 18 ml/min. In the isolated guinea pig hearts, simultaneous recordings of tension/pressure and surface electrograms (with electrodes close to the papillary muscle) were obtained following the methods described in our previous works (Costa et al. 2014; Ferreira de Mattos et al. 2017). The control results were obtained before and after the addition of LTB and subsequent washout of the toxin, as shown in Fig. 1 a, b, and c. In the controls, there were regular patterns of contraction, such as similar beat-to-beat amplitudes and homogeneous spontaneous regular heart rates. Upon the addition of 0.2 µg/ml LTB (which is the concentration reported to be near the IC50 of LTB-GM1 binding) (Minke et al. 1999), the patterns of contraction changed, such as the beat-to-beat characteristics, adopting an alternans pattern every two successive contractions. The effects observed upon application of LTB could be reversed after a wash-out period of a few minutes by reperfusion with Tyrode 1.8 Ca^{2+} solution. The kinetics of change is shown in Fig. 1d and e, for different LTB concentrations. Tension records showing cardiac alternans are shown in Fig. 1d. In Fig. 1e, at concentrations of LTB of 0.3 and 0.1 µg/ml, respectively, and using a fixed perfusion flow rate, the onset of action followed a sigmoidal time course with a time constant that varied between 1 and 2 min.

The steady-state dose-response curves for the mechanical effects of pressure/tension are shown in Fig. 2. In Fig. 2a, isolated heart contraction traces are shown at different concentrations of LTB. Note that LTB concentrations of 0.27 µg/ml and above show a clear mechanical alternans pattern when recorded in the isolated hearts. The ratios of the amplitude of two successive contractions during an alternans cycle were plotted against the toxin concentration, as shown in Fig. 2b. A Hill equation was fitted to the data in Fig. 2b, yielding an IC50 of 0.14 µg/ml. This IC50 value was surprisingly similar to that established for the binding of LTB to GM1 (0.12 µg/ml), according to the Sigma Product Information datasheet (PI E8656, LTB). Toxin action exhibited little cooperativity since the Hill number was near a value of one. The final ratio between the amplitudes of the peaks was near 0.2. It is interesting that the ratio of the amplitude of the second peak relative to the first peak diminishes with LTB increasing concentrations. Thus, by increasing the toxin concentration, the amplitude increased in the first peak of the tension transient compared with the second peak of the tension transient from the alternans cycle. The dependence of the ryanodine receptor type 2 (RyR 2) open probability with intracellular Ca^{2+} follows a bell-shaped curve (Balshaw et al. 1999). It has been reported that the bell-shape dependence with intracellular Ca^{2+} concentrations and the refractiveness of the RyR 2 probability may explain the observed cardiac mechanical alternans (Alvarez-Lacalle et al. 2013). In our experiments, LTB may promote an increased Ca^{2+} release from the sarcoplasmic reticulum (SR), and thus, it might enhance Ca^{2+} currents through voltage-gated-calcium-channels (VGCC) and/or the sensitivity of RyR 2 to Ca^{2+} ions, during the first peak. Upon the massive release of Ca^{2+} from the SR, Ryr2 channels are inactivated by Ca^{2+}, and hence, Ca^{2+} release is inhibited during the second peak and probably saturated at those LTB concentrations. As Ca^{2+} is removed from the sarcoplasm by SERCA, the inhibition is recovered for the next cycle to occur again. This is consistent with the

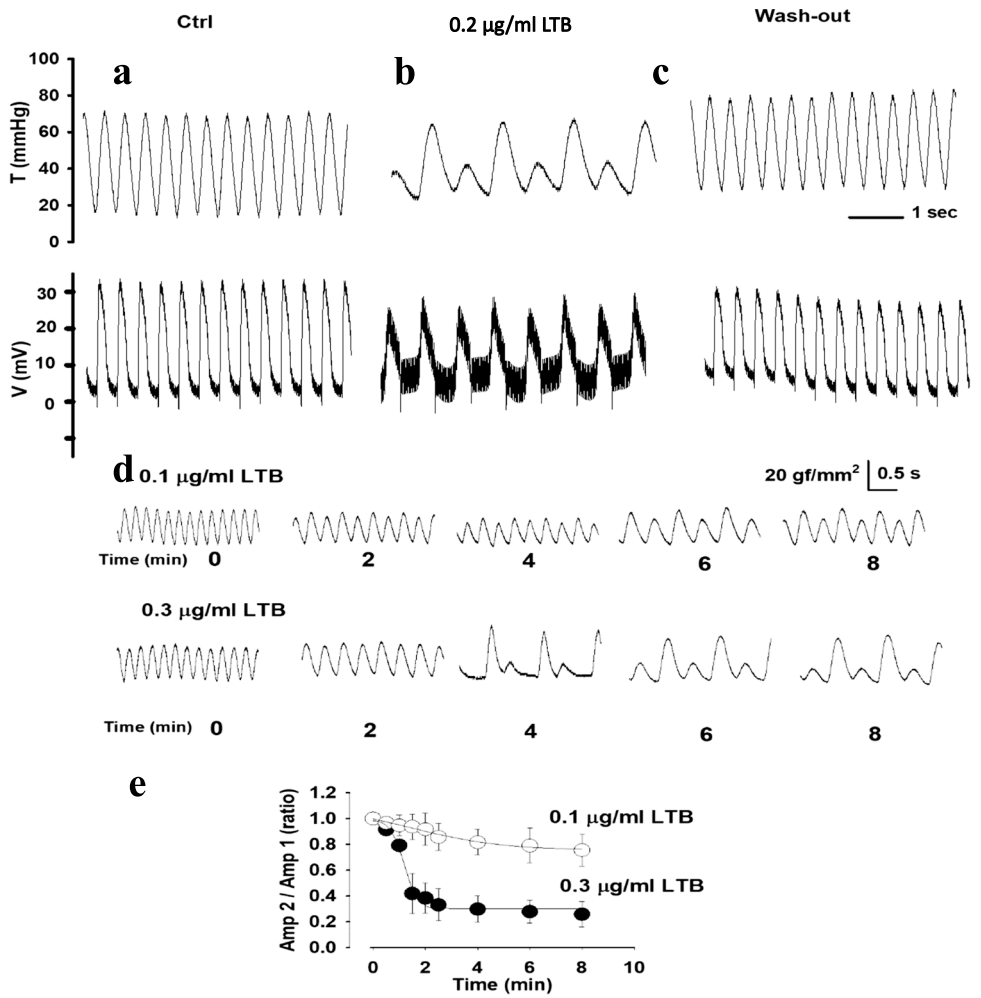

Fig. 1 The application of extracellular LTB to ex vivo guinea pig hearts promotes a pattern of mechanical and electrical alternans. **a** Simultaneous pressure/tension (*upper panel*) and surface electrogram records (*lower panel*) in control hearts. The pressure amplitude is maintained from beat to beat, and the heartbeat is regular on a beat-to-beat basis. **b** Simultaneous pressure/tension (*upper panel*) and surface electrogram records (*lower panel*) of hearts exposed to an extracellular perfusion of ~0.2 µg/ml LTB in Tyrode 1.8 Ca^{2+}. The pressure amplitude shows an alternating pattern that is not maintained in successive beats, in contrast to the control recordings. Concomitantly, the heartbeat is also altered and does not maintain a regular beat-to-beat pattern. **c** Wash-out of LTB-containing solution using 5 min of reperfusion with Tyrode 1.8 Ca^{2+} showing pressure/tension (*upper panel*) and surface electrogram (*lower panel*). There is almost complete restitution of the normal pressure amplitude and heartbeat, similar to that obtained in the control. The figure shows that LTB promotes mechanical and electrical alternans near the IC50 of binding of LTB to the GM1 receptor and its reversibility. **d** The kinetics of action of LTB on cardiac contraction at two different LTB concentrations in ex vivo guinea pig hearts with records of tension versus time obtained at 0, 2, 4, 6, and 8 min after the application of LTB at 0.1 µg/ml or 0.3 µg/ml. Tension units are in force grams per square millimeters (gf/mm^2). **e** The average plot of the ratio of the peak amplitudes (Amp 2/Amp 1) in alternans contractions during experiments similar to those reported in a is plotted versus time. Amp 2 is the measurement of the weak contraction after Amp 1, which is the measurement of the strong contraction. The results are obtained using 0.1 µg/ml (open symbols) or 0.3 µg/ml (filled symbols) extracellular LTB. The figure shows that the effect of LTB in promoting alternans contractions is dose and time-dependent. This is shown better at higher doses and times, as would be expected for a simple ligand-receptor binding dose-response. At both LTB concentrations, the effects can be fit reasonably well by a sigmoidal decay plot (solid line) (n=4)

proposal from Wei et al. regarding cardiac alternans (Wei et al. 2021). In Fig. 2c, the ratio of the duration of the half-time of the first peak of the alternans contraction and the duration of the alternans cycle is plotted against the concentration of LTB. This ratio increases with increasing doses of LTB, suggesting that alternans are more pronounced and that the first event becomes predominant in the alternans cycle with increasing LTB concentrations. This estimates the relative duration of the secondary event during the alternans cycle. Thus, we measured the duration of the mechanical response at 50% of the peak tension value during the first peak ($T_{1/2}$) and the duration of the total alternans cycle (TAtot), and then we calculated their ratio. Such a plot versus the concentration of LTB is shown

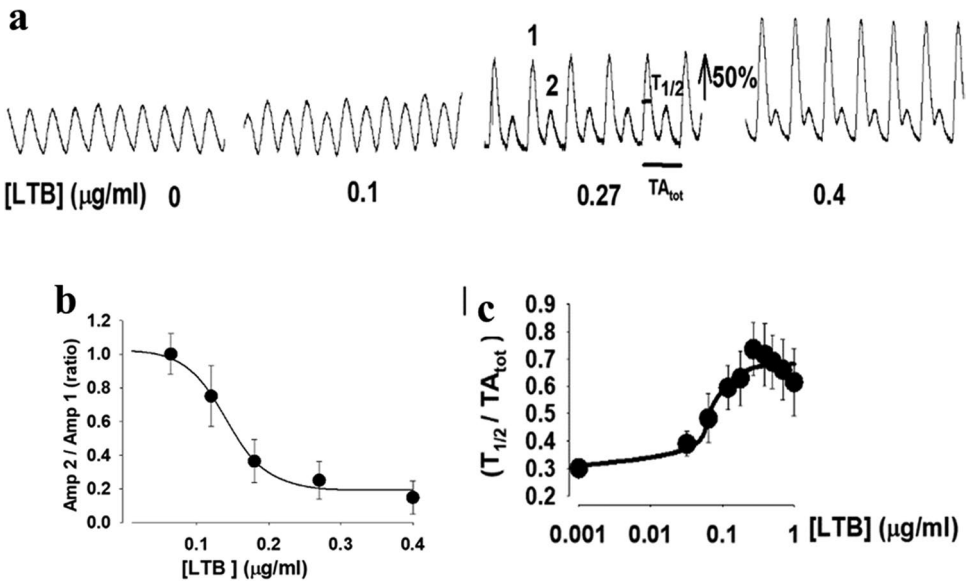

Fig. 2 Dose-response curves of mechanical alternans promoted by extracellular LTB in ex vivo guinea pig hearts. **a** Records of tension versus time were obtained at different LTB concentrations (indicated below the records). **b** The average plot of peak amplitude ratios during alternans at different LTB concentrations. Amp 2 is the peak amplitude of the weak contraction, whereas Amp 1 is that from the strong contraction. The solid line shows the best match of a Hill model to the results. The IC50 value from the Hill model fit (0.14 μg/ml) is very similar to that reported for the LTB-GM1 binding (n=4). **c** The average plot of the alternans duration ratios versus LTB concentration. $T_{1/2}$ is the duration of the first strong contraction at half of its amplitude. TA_{tot} is the duration of the whole alternans cycle. $T_{1/2}$/TA_{tot} represents the ratio of the duration of the first event at the half amplitude and total alternans cycle duration. The higher ratio indicates that the closest relationship between $T_{1/2}$ and TA_{tot} and that the first contraction has more weight and representation in the total alternans cycle duration. Only at high LTB doses does this ratio begin to slowly decrease, suggesting a saturation of the disrupting mechanism of the Ca^{2+} homeostasis. The solid line shows the best match of a Hill model to the results. The IC50 parameter is similar to that described for amplitudes found using 0.12 μg/ml LTB (n =4)

in Fig. 2c. The plot indicates that the duration of the secondary event decreases relative to the duration of a cycle with increasing LTB concentrations. The baseline level for tension was usually increased during the time course of the experiment. This result suggests increased Ca^{2+} release during the first peak and decreased Ca^{2+} reuptake during the second peak likely due to a change in the basal intracellular Ca^{2+} levels surpassing the ability of removal of Ca^{2+} from the myoplasm by the sarcoplasmic–endoplasmic reticulum calcium pump (SERCA). Alternatively, it is also likely that increasing LTB promoted higher intracellular Ca^{2+} levels promoting refractoriness or inactivation of RyR 2 during the second contraction in an alternans cycle. These hypotheses are not mutually exclusive. Cardiac alternans arises from dynamic variabilities in the electrical and Ca^{2+} handling cycling systems of the heart, found previously to ventricular arrhythmias and sudden cardiac death (Qu and Weiss 2023). Because of that, the electrical responses had to be studied with the mechanical responses in simultaneous recordings of tension and electrical response.

The pattern of modified mechanical alternans was also seen at the electrical level, after pairing the action potentials following the paired contractions during an alternans cycle. In Fig. 3a, the control experiment without alternans is shown to the left in the figure, and the experiment after the addition of 0.2 μg/ml LTB, with alternans, is shown to the right. The alternans cycles are shown in this figure for both mechanical and electrical responses. Although the electrophysiological changes seemed to be less marked or dramatic compared to the mechanical ones, they were also observed. The amplitude of the second contraction in the mechanical alternans cycle was always of less amplitude than the one seen in the first contraction. In the electrical response, the duration of the first and second electrical changes in the surface electrograms were always different as well. This was observed after measuring and comparing the ratio of the duration of the monophasic action potential at 80% of the amplitude during the first event of the alternans cycle ($T_{80\%}$), compared with the total duration of the alternans cycle (TA_{tot}). APD80 is suggested to be an equivalent measurement to $T_{80\%}$, and we define the duration of two successive events as the total duration or TA_{tot}. To relate the duration of the first event in comparison with the duration of the total event we measured the ratio ($T_{80\%}$/TA_{tot}). The higher its value indicates that the first electrical event has more weight concerning the total duration of the alternans cycle. We found that the ratio $T_{80\%}$/TA_{tot} became higher with increasing alternans and

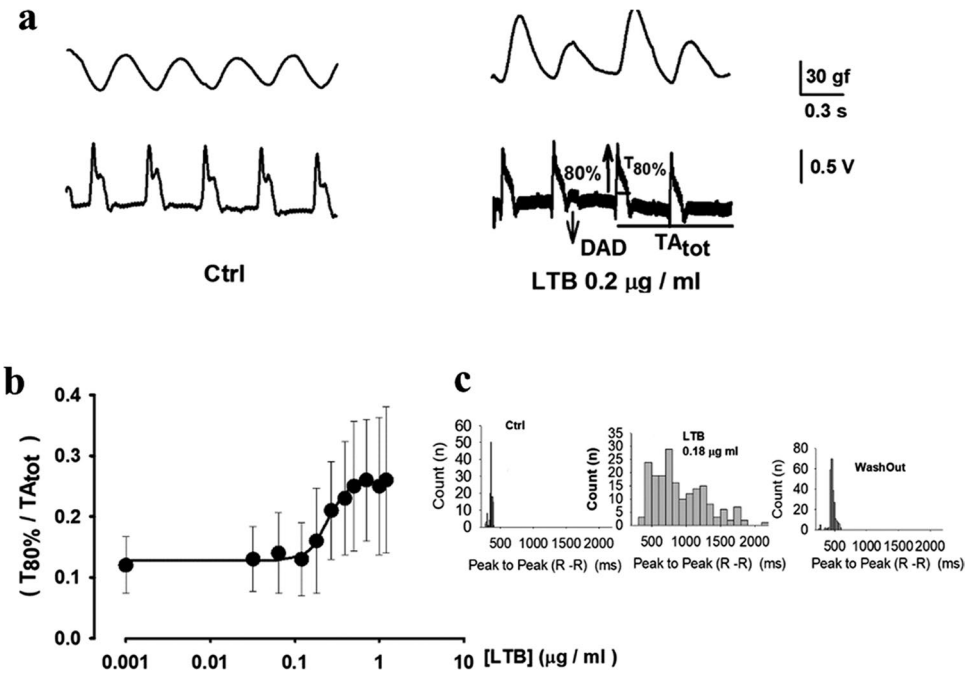

Fig. 3 Dose-response curve of electrical alternans and variability of heartbeats promoted by extracellular LTB in ex vivo guinea pig hearts. **a** Synchronous recordings of tension (*up*) and MAPs (*down*), in the papillary muscle. The *left panel* shows the control whereas the *right panel* shows LTB 0.2 µg/ml. The duration of the first electrical alternans event at 80% of its peak amplitude (roughly APD80) and the total duration of an alternans cycle are indicated in the figure for LTB. The arrow indicates a delayed after-depolarization (DAD). **b** The average plot of the alternans duration ratio is plotted versus LTB concentration. $T_{80\%}$ is the duration of the electrical event of the strong contraction at 20% from the baseline (80% from the peak, a similar notion to APD80, but here, it is done for monophasic action potentials, MAPs). TA_{tot} is the duration of the entire alternans cycle. $T_{80\%}/TA_{tot}$ is the measurement of the alternans duration ratio (first event/cycle). The higher the value of $T_{80\%}/TA_{tot}$, the more it represents the relative weight of $T_{80\%}$ in TA_{tot}. The solid line shows the best match of a Hill model to the results. The best-fit parameters of Hill's equations in both cases are similar to the IC50 of LTB binding (0.25 µg/ml) (n =4). **c** Histograms of the instantaneous heart rate in control, upon application of ~ 0.2 µg/ml LTB, and washout of LTB. The instantaneous heart rate measured from the R-to-R interval upon application of LTB diminished, increasing dramatically in its variability with time after application of LTB. The variability of the heartbeat was increased in the presence of the LTB toxin, and the effect was rapidly reversible after the washout of LTB

LTB concentrations. It is worth noting that in some recordings, pro-arrhythmogenic events similar to delayed afterdepolarizations (DAD) that are related to the dysregulation of intracellular Ca^{2+} homeostasis were observed (see DAD and arrow in the figure) (Fink et al. 2011). Figure 3b shows the relationship between exposure to LTB and response on the electrical alternans. The dose-response curve is represented as a semi-log plot of the ratio between the first event and the total duration during an alternans cycle versus the concentration of LTB (in µg/ml). The solid line shows the best match of a Hill model to the results. The data showed a similar IC50 to that reported for the mechanical response (IC50 approximately 0.25 µg/ml). Together, these results suggest that the changes in responses to tension can be correlated with electrophysiological phenomena. Thus, the effect of LTB in promoting alternans contractions appears to be in accordance at both the mechanical and electrical levels, suggesting a common mechanism may be responsible for the observed results. Finally, in Fig. 3c, it is shown that the beat-to-beat variability was highly increased by the toxin. To compute heart rate variability, and to plot histograms of the beat-to-beat time intervals variability, we used Kubios freeware from the University of Eastern Finland, Kuopio (Tarvainen et al. 2014). Histograms of the time intervals between beats at the beginning of the experiment (ctrl, left panel) during the administration of LTB (LTB, middle panel), and after the washout of the toxin (WashOut, right panel), are shown. The plots were obtained using Kubios software by plotting histograms of the number of events in a particular beat-to-beat time interval versus the duration of the time intervals between the amplitude or duration (between electrical peaks, R to R, in ms). The range of variability of these events in the control was quite small, as shown by the peak-to-peak duration in the range between 450 and 500 ms. The range of variability of the heart rate increased upon application of LTB, from 500 to almost 2000. After washout, the range of variability of the duration of the peak-to-peak events decreased to a range between 500 and 600 ms or more similar to the control. This increase in variability in the beat-to-beat ratio suggests a lack of coordination in the beating of

the whole heart and a propensity to get anomalous rhythm centers that could potentially lead the heart to ventricular fibrillation and sudden cardiac death. With this uncoordinated electrical signaling, the heart also lost its ability to contract synergistically on a beat-to-beat basis.

The presence of extracellular LTB at those concentrations promotes cardiac alternans in a reversible way, presumably by GM1 binding because of the specificity of LTB binding to this receptor, because of the concentrations found to have an effect promoting alternans are strikingly similar to those reported for LTB-GM1 binding, and, finally, because of the reversibility of the effect (Minke et al. 1999). The results reported in isolated hearts with acute exposure to LTB show that the toxin promotes cardiac alternans at doses like the IC50 reported for GM1 binding of this toxin. This was a correlated pattern of electrical and mechanical alternans observed with the extracellular application of LTB. GM1 is abundant, and it has several actions in the heart (Lodovici et al. 1993; Marengo et al. 1998). Cardiac alternans has been linked to arrhythmogenesis and sudden cardiac death (Costantini et al. 2000; Laurita and Rosenbaum 2008; Rosenbaum et al. 1994; Walker and Rosenbaum 2005; Wilson and Rosenbaum 2007; Wilson et al. 2006). A beat-to-beat alternans pattern was suspected to arise from changes in intracellular Ca^{2+} cycling and alternatively from action potential duration restitution (Sarusi et al. 2014; Wilson et al. 2006). Several conditions that are able to promote heart failure either intrinsically such as hypothermia, hypo or hypercalcemia, hypercapnic acidosis, ischemia, hypertrophy, or extrinsically, such as β-adrenergic agonists, digitalis, and calcium channel antagonist, can elicit cardiac alternans (Euler 1999; Qu and Weiss 2023). The gut microbiome seems to play an essential role in the progression to disease of individuals infected with ETEC *E. coli*, especially in children in low- and middle-income countries (Higginson et al. 2022). These findings, joined to these particular results, indicate that the effect of LTB in GM1 cardiac gangliosides eliciting cardiac alternans being able to promote sudden cardiac death is a plausible hypothesis worthwhile to be explored.

This set of results supports the view that bacterial toxins can have detrimental effects on the heart and contribute to the development of cardiac dysfunction, as we have stated before. Bacterial toxins can cause inflammation, vascular permeability, and organ malfunctions, including the heart (Guichard et al. 2012). Cardiac alternans reflects some stages of heart failure that usually precedes more important arrhythmias (Kulkarni et al. 2019). In the context of heart failure, altered gut microbial communities can contribute to the disease through bacterial translocation or affecting metabolic pathways (Chen et al. 2019). Our results are consistent with previous findings showing that the composition of the gut microbiota in people with heart failure is different from those with a healthy status (Chen et al. 2019). Bacteria living in the gut secrete molecules that must penetrate the intestinal epithelium or the surface cells of the host. We suppose that LTB, like Cholera toxin, bind to GM1 gangliosides located on the outer leaflet of the apical membrane in intestinal epithelial cells (Wernick et al. 2010). Besides binding to membrane components like LTB, some bacterial toxins can form pores (Wang et al. 2017), while others may involve lipoprotein binding and inflammation modulation (Kilpatrick et al. 2007) or the promotion of autophagy in infected cardiac cells (Gurusamy et al. 2009). Whole cholera toxin (A and B fractions), injected into rat tails, promoted cardiac arrhythmias leading into ventricular fibrillation and an increment of cAMP through activation of guanine nucleotide regulatory proteins (Huang and Wong 1989). Those experiments were performed with the whole toxin and not the B fraction. Regarding the whole cholera toxin, it has been also reported to change triacylglycerol lipase activity and cardiac metabolism when injected into heart rats (Miller et al. 1987). Our set of experiments is different to those using cholera toxin, because we have used only the B fraction from *E. coli*, applying it extracellularly to guinea pig isolated hearts. The effects of LTB in isolated hearts have not been thoroughly explored, except for some global work in zebrafish, where it was reported that LTB was able cause systemic impairment of various organs, including the heart (Henrique et al. 2021). It is worth mentioning that the epidemiological association between ETEC *E. coli* and sudden cardiac death has been reported several times since the 1990s, but no phenomenological link was established (Bettelheim et al. 1989; Bettelheim and Goldwater 2015; Bettelheim et al. 1990; Murrell et al. 1993). It is interesting that the toxigenicity appeared to be relatively labile regarding the temperature (Bettelheim et al. 1990). The results presented here might offer the phenomenological explanation that was lacking from the epidemiological studies mentioned above,

After reviewing and reporting experimental evidence in isolated hearts, regarding extracellular LTB-promoting cardiac alternans, we examined the effects of increasing doses of LTB on action potentials and ionic currents in isolated cardiomyocytes.

LTB enterotoxin from *E. coli* promotes electrical and mechanical alternans and differentially affects the main ionic currents in isolated cardiomyocytes from guinea pigs

To test if the observations seen at the level of the whole heart were due to changes in conduction patterns and syncytium functioning of the heart and to ascertain the main electrophysiological targets of LTB at the cellular level, we recorded action potentials and ionic currents from isolated cardiomyocytes.

Cardiomyocytes were isolated following the protocol developed by Ferreira et al. (Ferreira de Mattos et al. 2017; Ferreira et al. 1997a), which was adapted from Mitra and Morad (Mitra and Morad 1985).

Action potentials were recorded in a whole-cell configuration following a similar procedure described by Kato et al. (1996), under the current-clamp configuration, as shown in Fig. 4a. The addition of 0.2 µg/ml of the LTB toxin in the extracellular solution changed the amplitude and duration of the action potentials. The amplitudes were reduced by an average of 20 ± 4%, and the duration was diminished by 44 ± 4% or 6 ± 4% at APD20 or APD80, respectively. The duration was measured at 20% and 80% of its total amplitude (approximately 100 mV), and this was measured from the overshoot to the resting potential of 110 ± 10 ms and 270 ± 18 ms, respectively (APD20 and APD80, respectively). These findings indicated that the duration of the plateau was diminished by the application of LTB, although the duration of the repolarization of the action potential was only mildly affected. In the control experiments without the toxin, single cardiomyocytes were used for comparisons between two successive contractions and action potentials. When a paired group of pulses were applied at 3–4 Hz to reproduce the normal heart rate of the guinea pig, in the presence of LTB, an electrophysiological pattern of alternans (amplitude and duration of the action potentials) occurred, similar to those reported for the whole heart (Fig. 4b). Action potentials and contractions using control cultures and cultures containing 0.2 µg/ml LTB were compared in bar plots (Fig. 4c). The ratios of the action potential amplitudes between successive contractions in LTB-treated and control cultures were very similar (near 0.8 or 80 ± 15% in terms of percentage). This ratio is modified more when the comparison was done between contractions (near 0.6 or on a percentage basis, 60 ± 12%). This analysis demonstrates that the alternans pattern promoted by the toxin in the whole heart can be observed in individual isolated cardiomyocytes when exposed to similar concentrations of LTB toxin.

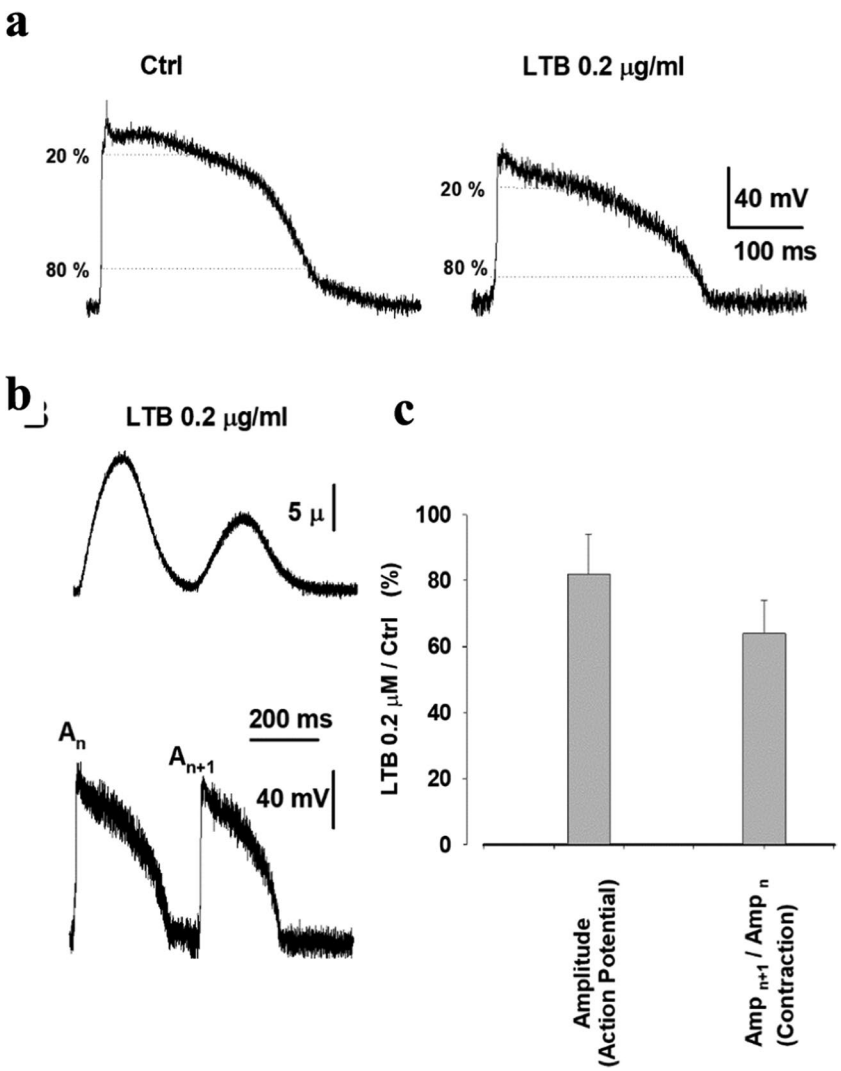

Fig. 4 Effect of 0.2 µg/ml extracellular LTB on action potentials and contractions recorded from isolated ventricular cardiomyocytes. **a** The application of LTB toxin changed the amplitude of the action potential in single cells (APD20 and APD80 are shown). APD20 was more affected by the toxin than APD80 where the duration of the action potential is slightly changed, possibly due to an enhancement of the peak of ICa and/or partial inhibition of the Ito K^+ current by the toxin. **b** The mechanical and electrical alternans phenomena are seen in isolated cardiomyocyte cells exposed to LTB when pulses were applied at a rate of 2–3 Hz at a concentration of 0.2 µg/ml LTB. **c** The average plot of the effect of LTB on single cells (action potential and contraction/shortening). The data were plotted as bars for each situation. The effect of the toxin on action potential amplitude (A_{n+1}/A_n) and the amplitude of shortening between consecutive pulses are shown for n=3 cells

These results show that the alternans patterns of contraction seen at the level of the whole organ are a consequence of alterations promoted by the toxin in isolated cardiac cells because those patterns are also seen in isolated cardiomyocytes exposed to LTB. This is consistent with the hypothesis that LTB binds to GM1 promoting the changes at the cellular level in cardiomyocytes, as gangliosides are known to be important modulators of function in excitable cells (Busselberg et al. 1989), and that it was found that the permeability to Ca2+ in cardiac cells can be modulated by sialic acid-containing gangliosides located in the sarcolemma (Marengo et al. 1998).

The decrement of action potential duration in the second action potential in an alternans series promoted by LTB reported in Fig. 4 could be the result of changes in ion channel activity promoted directly or indirectly by the toxin. There is a tight relationship between heart failure and ion channel electrophysiology (Marbán 1999). Thus, to better understand the voltage changes, we studied the effects of LTB on ionic currents under a whole-cell patch clamp.

Figure 5 shows the results of applying extracellular LTB to the main ionic currents present in ventricular cardiomyocytes. Figures 5 a, b, and c show the pulse protocol and Na^+ currents (INa) obtained in control and in 0.2 µg/ml LTB. To avoid the spontaneous shift of Na channel voltage-dependent gating (availability), we choose a holding potential of −110 mV (Hanck and Sheets 1992; Maltsev and Undrovinas 1997). Thus, if any decrease in Na amplitude in the presence of LTB is observed, it could not be explained by the time-dependent shift of the steady-state availability curve (Hanck and Sheets 1992; Maltsev and Undrovinas 1997). To determine the effect of LTB on INa, NaCl was also reduced to 50 mM to obtain a better voltage clamp. We also substituted 90 mM extracellular NaCl with TEACl. Though they are hard to get, INa has been recorded under extracellular Na^+ concentrations of 50 mM or more with the whole-cell patch-clamp technique (Tanaka et al. 1994; Wang et al. 2009). Blocking of K^+ channels was achieved by incorporating high intracellular Cs^+, high extracellular TEA, and the addition of 5 mM 3,4 diamino-pyridine (Jeevaratnam et al. 2018). The osmolarity of the intracellular solution was kept constant with 140 mM CsCl. The blocking of Ca^{2+} channels was achieved by the addition of 5 µM dihydropyridine. Capacitive currents were subtracted using a standard P/4 protocol. In Fig. 5 b and c, the INa IV curve traces and plots are shown in reference and LTB. Plots are shown in Fig. 5c showing a stable increment and not an abrupt rise of the peak INa with membrane voltage, to make sure we do not have "escape" clamp problems (Carmeliet 1987; Pásek et al. 2008; Wasserstrom and Vites 1999). The data are consistent with a minor but significant effect of LTB on the gating mechanism of cardiac Na^+ channels, similar to what it has been observed in hypercholesterolemia (C. C. Wu et al. 1995). It is interesting that GM1 located through *Cholera toxin* (CTX) binding is preferentially located in cholesterol-enriched membranes (Orlandi and Fishman 1998; Wolf et al. 1998). GM1 located through this method promotes a reorientation of the membrane cholesterol that may change the physicochemical properties of the membrane and influence transmembrane proteins (Rondelli et al. 2012). The fast Na^+ channels or Nav1.5 channels traffic together to the sarcolemma with the K^+ inward rectifier Kir2.1 channel (Ponce-Balbuena et al. 2018), and it is associated with these lipid rafts enrichened in cholesterol through its β subunit (Cortada et al. 2021). Alternatively, these results, especially a slower inactivation rate, could be explained by phosphorylation through the PTK pathway stimulated by the GM1 toxin binding (Ahern et al. 2005). This effect may partially account for the changes in excitability patterns and arrhythmogenesis observed after the extracellular application of LTB, and it does not seem to be the main mechanism of LTB arrhythmogenesis. The time control of the course of action and washout of LTB on INa currents is shown in Supp. Fig. 2. To summarize, INa was decreased by extracellular LTB, consistent with the results showing that Na^+ currents were greatly affected by LTB B subunits that reduced neuronal excitability and conduction in visceral and baroreceptor afferent nerve fibers (Qiao et al. 2008).

The effects of LTB on Ca^{2+} currents in myocardiocytes were also explored, and the results are presented in Fig. 5 d, e, and f. To study the effects of LTB on Cav1.2 currents (ICa), a prepulse of −40 mV for 50 ms was used to modify the resting potential of −80 mV. This was done to inactivate sodium channels (Mangold et al. 2017). The application of 0.2 µg/ml LTB promoted a change in the current peak and a change in the fast current inactivation rate of ICa (Fig. 5d). The increment observed at the current peak amplitude for pulses to −10 mV was greater by an average of 20 ± 4%, whereas an extension of inactivation for 250 ms pulses was augmented by 40 ± 5% (Fig. 5e). The IV curve normalized for control and LTB is shown in Fig. 5f, and it looks like it is shifted ~20 mV towards more negative potentials, being consistent with some sort of charge screening effect (Bers and Peskoff 1991). Though the IV curve is normalized in both cases, the amplitude is increased by approximately 5–10% in absolute terms by LTB. Because of this, the same voltage used in the figure will increase its current and enhance calcium-dependent inactivation when LTB is present. Although these are subtle changes in ICa, they might explain the effects observed by altering intracellular Ca^{2+}, and they may well also contribute to the alternans pattern of contraction, as it will promote a transient Ca^{2+} release from the RyR2 in the SR (Eisner et al. 2017). Subtle changes in ionic currents are known to correlate with Ca^{2+} release from the SR. Another important issue from this result is that ICa inactivation is significantly increased by LTB. Thus, ICa might be still partially inactivated and not fully recovered

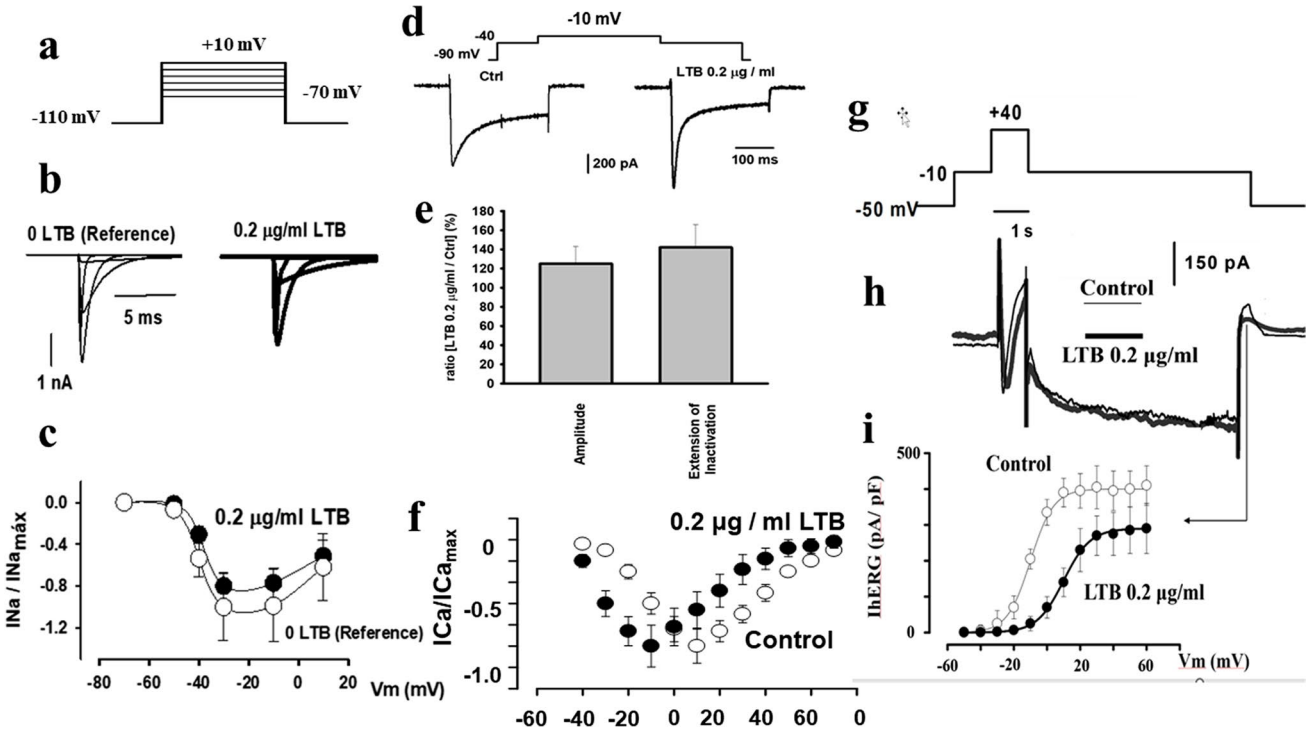

Fig. 5 The main ionic currents from isolated guinea pig cardiomyocytes are affected by the addition of extracellular 0.2 µg/ml LTB. **a** Pulses to explore INa, applied from a holding potential of −110 mV to avoid any spontaneous shift of INa (Hanck and Sheets 1992). **b** Current-voltage records of INa in reference (*left*, thin traces) and in 0.2 µg/ml LTB (*right*, thick traces) elicited by the pulse protocol shown in **a**. No escape clamp problems were observed in the records obtained. To avoid clamp problems, extracellular Na^+ was lowered to at least 50 mM. Capacitive currents were eliminated by standard procedures (Ferreira 1997a, b; Ferreira et al. 2003). **c** Normalized peak INa current-voltage curve in reference and LTB. The increment of INa towards a maximum peak around −30 mV is smooth and not abrupt indicating that the effects observed are not artifactual due to escape problems. LTB diminished slightly INa at all voltages (n=5). **d** ICa recorded after inactivation of INa and IK blockage in control (*left panel*) and after application of the toxin (*right panel*), using applied pulses from −40 to −10 mV. Both ICa peak and inactivation rates were increased by the extracellular application of 0.2 µg/ml LTB (*upper trace*). **e** The average plot of the ratio LTB/Ctrl observed on ICa peak amplitude and extension of inactivation for 300 ms pulses. In the presence of the toxin, there were increments in ICa peak amplitude (25%), and the extension of inactivation was increased (42%). Both changes were significant (n=3, p=0.05). **f** Normalized IV curves of ICa in control and in LTB. Normalizations were done for each situation independently. In LTB, the curve seems to be shifted towards more negative potentials. The results indicate that calcium currents increase their peak and their inactivation rate after the application of 0.2 µg/ml LTB in isolated ventricular cardiomyocytes. **g** The usual protocol to isolate both delayed outward currents was used following published procedures (Heath and Terrar 1996; Jo and Lee 2010; Sanguinetti and Jurkiewicz 1990). The first repolarization measures IKr (hERG), while the second one estimates IKs (KCNQ). **h** The recordings for the protocol shown in **a** are displayed. The thick trace represents the recording with 0.2 µg/ml extracellular LTB, while the thin trace represents the recording in controls. LTB reduces both outward currents (n=3). **i** IV curves for the peak of hERG current upon repolarization to −50 mV. The curves were obtained in control and in LTB. The line and arrow indicate the peak where the hERG current was measured. The example was from a pulse from −10 mV. LTB reduces the hERG currents and shifts the curve to towards more depolarized potentials. The solid line represents the best fit of a Boltzmann equation to the data (n=3). The results suggest that the application of 0.2 µg/ml extracellular LTB promotes changes in slow outward K^+ currents in isolated ventricular cardiomyocytes. The set of results reported in this figure indicate that LTB is able to promote changes in all major ionic currents responsible for cardiac action potentials and excitability

from inactivation, if an AP is elicited closer to the previous one, contributing to an alternans pattern as well. This is consistent with results reported by several groups (Hopenfeld 2006; Lai et al. 2020; Mahajan et al. 2008).

A possible explanation could be related to a shift towards more negative potentials promoted by screening of positive charges by the presence of GM1 toxin binding. We have made molecular dynamics simulation and analysis, that show that GM1, possibly increased with toxin binding, increases the amount of cation concentrations next to the membrane (see final interpretations at the end).

An alternative and non-exclusive explanation to the former one of the effects of LTB observed at the level of Cav1.2 currents could be explained if the toxin enhanced the activity of the calmodulin pathway. CaMKII is known to increase arrhythmia and cardiac function (Glynn et al. 2015). It can increase either ICa inactivation or facilitation (Bers and Morotti 2014; Peterson et al. 1999; Zhao et al. 2014). It

also has effects especially on the late Na current shifting its activation towards more negative potentials (Ashpole et al. 2012). In agreement with these results, calmodulin binds to the GM1 receptor, and the stimulation of the GM1 receptor increases calmodulin activity (Fukunaga et al. 1990; Higashi et al. 1992). These results were similar to those reported for butanedione, an oxime that dephosphorylates the L-type calcium channel (Ferreira et al. 1997a, b). They also suggested that most of the effect on ICa was due to the fast inactivation mechanism related to calcium-dependent inactivation, even though there seems to be an interplay between calcium and voltage-dependent inactivation (Ferreira et al. 2003; Grandi et al. 2010). This view is also consistent with other series of experiments that we have performed with heavy metals in the heart (Ferreira de Mattos et al. 2017; Ferreira et al. 2022) and correlations between gating currents and ionic currents (Ferreira et al. 2001).

To summarize, ICa through Cav1.2 channels were also affected by LTB, but in a distinct way than INa. The peak of ICa was mildly increased upon the addition of extracellular LTB, but the effects of promoting ICa inactivation were observed for most of the duration of ICa, especially for fast inactivation (Ferreira et al. 2003; Peterson et al. 1999). The effects of LTB and B-type toxins from the AB_5 family on calcium channels have been reported in other cell types (Carlson et al. 1994; Hilbush and Levine 1992; Slomiany et al. 1992). The relativity mild effects of LTB on Cav1.2 currents observed here were consistent with the results obtained in cardiomyocytes by Marengo et al. (1998) and in isolated preparations of Ca^{2+} channels by Slomiany et al. (Marengo et al. 1998; Slomiany et al. 1992). The results can be explained either by the charge screening effect and also by activation of the calmodulin pathway. From our experiments, we cannot rule out the stimulation of Trp-like channels upon LTB binding, and this could contribute at least partially to the observed results.

Finally, to gain information about K^+ currents, currents were recorded adding 30 µM extracellular TTX, 5 µM nifedipine to block INa and ICa (guinea pigs do not have important Ito K^+ currents), respectively. Under these conditions, the remaining current is mostly a K^+ current. We applied a voltage-clamp protocol using almost instantaneous voltage jumps to eliminate the capacitive currents with standard P/4 protocols. Slow voltage-dependent potassium currents (IK) important for repolarization were recorded with 3-s pulses to −10 mV and after 1-s-long pulses to +40 mV from a holding potential of −50 mV. This holding potential was used to eliminate INa in addition to TTX, and we ended up with repolarization to the −50 mV holding potential after the 3-s pulse to −10 mV (see pulse protocol, Fig. 5g). To minimize the possible interference of inward rectifier K^+ currents, 5 mM CsCl was added to the extracellular solution. The extracellular Ca^{2+} necessary to obtain the patch-clamp seal was lowered to 1 mM to avoid most of the interference caused by the very fast inward current tail that is mostly lost due to the low sampling rate we used to record the delayed K^+ currents. Slow outward potassium currents at the end of the 1-s pulses and tails at −10 mV represent mostly currents passing through the fast delayed rectifier hERG channel (IKr). The slow outward currents after the 3-s pulses to −10 mV that returned to the holding potential represent mostly the slow delayed rectifier potassium currents (IKs) (Heath and Terrar 1996; Jo and Lee 2010). The amplitude and kinetics of delayed rectifier K^+ currents (IKr and IKs) were decreased upon the addition of extracellular LTB (see the thick black trace in Fig. 5h). The observed results in terms of potassium currents were consistent with those reported for action potentials in single cells, having a longer AP in the first of two successive AP (see Fig. 4). In Fig. 5i, the IV curve for the peak of the hERG current was plotted versus the membrane potential previous to the repolarization to −50 mV in control and in LTB. LTB diminishes the hERG currents shifting the IV currents to the right. The solid lines represent the best fit of a Boltzmann equation to the data. Note that the maintenance current for holding the potential at −50 mV is diminished by the toxin. This could imply that the inward rectifiers of the heart (Kir2.1) are also inhibited by LTB. If this occurs by down-regulation of PIP2, as Kir2.2 activity is critically dependent in PIP2, these finding would be consistent with that work hypothesis as well (Huang et al. 1998).

In contrast with Na^+ and Ca^{2+} currents, there are fewer reports and studies on the effects of LTB and gangliosides on K^+ channels. In general, the outward currents carried by K^+ channels were mildly diminished by LTB, presumably through the delayed rectifier channels (KCNQ or HERG). This may explain changes in alternans APD by toxin binding. The first AP in two successive alternans is longer and prone to long QT intervals due to this effect. This effect, in turn, could partially promote malignant arrhythmias that could lead to sudden cardiac death (Antoniou et al. 2017; Zareba and Cygankiewicz 2008). With our results, however, we cannot rule out additional effects on inward rectifier channels (Kir). It is known that the hERG channel is a direct or indirect target of many drugs, pathways, and infectious diseases that could lead to arrhythmogenesis (Ferreira et al. 2021; Fossa et al. 2004). It is interesting that cholesterol and GM1 tend to be colocalized (Lozano et al. 2013). The hERG channel has been found at higher densities in domains containing cholesterol in neurons (Jiménez-Garduño et al. 2014). Finally, cholesterol tends to down-regulate the activity of the channel making it pro-arrhytmic (Balijepalli et al. 2007; Balijepalli and Kamp 2008; Chun et al. 2013). It is known that GM1 forces the redistribution of cholesterol in membranes (Rondelli et al. 2012). The effect of cholesterol in the hERG channels seems to be related to a down-regulation of phosphatidyl-inositol-4,5-biphosphate (PIP2), which

in turn diminishes the current through these channels (Chun et al. 2010). It is conceivable that hERG and KCNQ currents could be affected by GM1 and toxin binding in a similar way to what we reported for INa in Fig. 5a.

The alterations in inward and outward currents may explain the pro-arrhythmogenic effects of extracellular LTB. The results obtained are consistent with what it has been experimentally reported for Na, Ca, and K currents during cardiac alternans (You et al. 2021). They are also consistent with theoretical models proposed for alternans, where alternative uncoupling of Cav1.2 Ca^{2+} channels from Ryr 2 subunits, due to inactivation, could explain these phenomena (Hoang-Trong et al. 2021). The LTB toxin promotes an imbalance in the plateau and repolarization phase of the action potential where pro-arrhythmogenic events can arise. Because of its effects on the ionic currents, LTB should promote QT imbalance, which has also been statistically correlated with alternans and sudden cardiac death (Maury et al. 2012; Panicker et al. 2012; Tse et al. 2017).

Bacterial toxins can modulate membrane properties through direct or indirect mechanisms (Eidels et al. 1983; Lesieur et al. 1997; Ostolaza et al. 2019). Pore-forming toxins (PFT) are a way to get direct interference with membrane permeabilization properties (Dal Peraro and van der Goot 2016). They have analogous proteins in vertebrates and other eukaryotes, with very similar structures, termed, pore-forming toxins (PFT) (Dal Peraro and van der Goot 2016). Usually, they can be classified into two large groups, α barrel and β barrel, according to the predominant secondary structure of their transmembrane regions (Iacovache et al. 2010; Lesieur et al. 1997). All of them have before reaching their target cells, inactive monomeric, water-soluble structures, that when they reach the target cell membrane, interacting with sugars, lipids, and proteins receptors, undergo a change to a transmembrane protein, permeable to several cations and other molecules (Dal Peraro and van der Goot 2016). This interaction needs receptors that are usually placed in lipid rafts rich in cholesterol or sphingomyelin (Dal Peraro and van der Goot 2016; DuMont and Torres 2014; Los et al. 2013). Then, toxin oligomerization takes place, forming a ring-shaped pore that finally communicates intracellular with extracellular media (Dal Peraro and van der Goot 2016). In this way, they alter membrane permeability and action potentials of excitable cells because they are permeation pathways themselves.

Bacterial toxins that form pores in the heart can have detrimental effects on cardiac function and contribute to various cardiac diseases. One such toxin is pneumolysin (PLY), which is produced by *Streptococcus pneumoniae* (Boulnois et al. 1991). PLY is a member of the β barrel family described previously and the main virulence factor of *Streptococcus pneumoniae* (Anderson et al. 2018). It is a cholesterol-dependent pore-forming toxin that kills cardiomyocytes in vitro and disrupts cardiomyocyte contractility because of alterations in membrane permeability by direct mechanisms, so circulating PNY is a potent inducer of cardiac injury during infections by *Streptococcus pneumoniae*, which are unfortunately common (Alhamdi et al. 2015; Zivich et al. 2018). Some of these PFT toxins may be associated with sepsis (a systemic inflammatory response following bacterial infections), having a significant role in the damage of multiple organs, among them, the heart compromised (Abrams et al. 2022). Though there are variations, most of the clinical presentations of these PFTs altering membrane permeability in cardiac myocytes tend to be more dramatic than those from toxins that indirectly affect membrane permeability (Eidels et al. 1983; Los et al. 2013).

Our results are consistent with those of bacteria that indirectly alter membrane permeability through receptor binding, and that, in turn, may impact cell excitability in the case of the heart, at various levels. It is interesting that though not common, some reports of cardiomyopathy due to *Clostridium* infections have been made (Virk and Inayat 2016). The Rho kinase pathway is inhibited by *Clostridium* toxins (Popoff and Poulain 2010). This pathway is of high relevance to cardiac physiology (Dai et al. 2018). Besides promoting a regulation of the contractile machinery, the Rho pathway is also important in modulating membrane permeability through several ion channels (Jin 2009). The amount of GM1 in membranes can change dramatically the responses of the membranes. In fact, in hereditary diseases known as gangliosidosis, there is a lipid storage disorder where they get accumulated in the lysosomes from neurons mostly, leading to developmental anomalies of the affected individuals (Nicoli et al. 2021). GM1 is prominent especially in membrane lipid microdomains. The binding of B subunit from cholera toxin diminishes INa in neurons, consistent with our findings (Qiao et al. 2008). Interestingly, there are reports that the B subunit of cholera toxin activates L-type Ca^{2+} currents in neuroblastoma cells, consistent with our report (Carlson et al. 1994). Besides local perturbation upon binding to toxins, there could be several downstream pathways that are changed that in turn can affect ionic permeabilities of the membrane at multiple levels, like the ones reported in this paper (Ledeen and Wu 2015).

We did not evaluate the effects of LTB on other known currents in ventricular myocytes, which can contribute in a smaller way to the observed effects on the function of the organ. For example, using our general current recording procedure, we did not evaluate the possible effect of LTB binding to Trp or SOC Ca^{2+} permeable channels or chloride currents as well as aquaporins, gap junctions, NCX transporters, and pumps. The differences in the currents recorded in control and LTB-treated samples, with the more obvious channels blocked by ion substitution, prepulse, or channel blockers, suggested that Trp/SOC channels are also affected,

though not eliminated, by LTB. We finally explored if LTB promoted changes in intracellular Ca^{2+} dynamics in isolated cardiomyocytes.

LTB changes intracellular Ca^{2+} dynamics in isolated cardiomyocytes

The results reported here on the currents and channels of cardiomyocytes are due to LTB B-subunit-GM1-binding that directly or indirectly affects cells. In the alternans pattern, there is usually an alteration of the dynamics and management of intracellular Ca^{2+} that, in turn, can affect cellular currents (Wagner et al. 2015). Thus, we explored the effects of LTB on intracellular Ca^{2+} concentrations and distribution with fluorescent Ca^{2+} dyes. It is well known in neurons and other cell systems that GM1 ganglioside can regulate transmembrane signaling, which in turn can alter intracellular calcium dynamics (Ravichandra and Joshi 1999). Acute exposure of LTB to cardiac cells might affect transmembrane signaling, leading to a loss of coordination of intracellular Ca^{2+} dynamics. It has also been established that GM1 gangliosides and drug binding to these receptors are important modulators of PTK activity and Ca^{2+}-dependent protein kinases (Bremer and Hakomori 1984; Bremer and Hakomori 1984; Hilbush and Levine 1992; Kim et al. 1986). In addition, PTK activity and Ca^{2+}-dependent protein kinases are important modulators of ion channels and transporters in the plasma membrane as well as intracellular Ca^{2+} dynamics from intracellular stores (Lu et al. 1994; Marks 1997; Nie et al. 2007). Taking the above into account and also that alternans mechanisms are likely due to disturbances in the modulation of intracellular Ca^{2+} dynamics (Weiss et al. 2006), we explored the consequences of acute exposure to LTB on intracellular Ca^{2+} concentrations and distributions in isolated cardiac myocytes. An increment in intracellular Ca^{2+} may in turn promote another pro-arrhythmogenic event like delayed afterdepolarizations (DAD) (Tveito et al. 2012).

Since intracellular Ca^{2+} dynamics are critical for cardiomyocyte functioning, and they are also highly modulated by cardiomyocyte electrophysiology, we studied the effects of the extracellular application of LTB on global intracellular Ca^{2+} concentrations using imaging with Ca^{2+}-sensitive fluorescent dyes limited to the isolated cardiomyocyte boundaries over time (see Supp. Fig. 3). Ca^{2+} imaging was obtained from single isolated cardiomyocytes loaded with Fluo-3-AM or Fluo-4-AM (Molecular Probes, Invitrogen, Carlsbad, CA; USA and AAT, Sunnyvale, CA, USA) in a confocal microscope, following standard procedures described by Guatimosim et al. (2011).

Figure 6a shows the intracellular Ca^{2+} distribution in isolated cardiomyocytes visualized with a confocal microscope without extracellular stimulation (resting) in a control culture and culture after treatment with 0.2 µg/ml LTB. The green fluorescence in the transillumination image of the cardiac myocyte represents higher concentrations of intracellular Ca^{2+}. Below the transilluminated images are only the Fluo-3AM images corresponding to those images above. In Fig. 6b, the relative fluorescence of Fluo-3AM bound to Ca^{2+} $(\Delta F/F)^{+}$ is plotted for the control and LTB-treated cells shown in Fig 6a. Occasionally, spontaneous Ca^{2+} release was observed, though this situation was more frequently observed in those cells exposed to the toxin. The addition of 0.2 µg/ml extracellular LTB increased the average basal intracellular Ca^{2+} concentration (Fig. 6b). The amplitude of the intracellular Ca^{2+} spontaneous oscillations is higher, and the variability between the amplitude of the oscillations was larger in the LBT-treated than in the control cells. The levels of intracellular Ca^{2+} in LTB were high enough above control levels to occasionally observe a contraction by the cardiac myocyte (Fig. 6b). These spontaneous local Ca^{2+} oscillations happened around an average resting level of Ca^{2+} for the whole cell which was bigger in LTB than in control. This result, in general, follows classical works such as Cheng et al. (1996) and Lopez et al. (1995). The global intracellular Ca^{2+} reports rely on the existence of local events such as spontaneous calcium sparks and/or waves in diastolic cardiomyocytes like those shown in Fig. 6a. They produce changes in the measured average intracellular Ca^{2+} bound to Fluo-3AM, observed as fluorescence peaks above an average (Cheng et al. 1996; Lopez et al. 1995). Thus, the addition of 0.2 µg/ml extracellular LTB dysregulated the normal homeostatic concentration levels and oscillations of intracellular Ca^{2+} under resting conditions without extracellular stimulation (see resting in Fig. 6 a and b), resulting in increased concentration of basal intracellular Ca^{2+}, as well as more pronounced local Ca^{2+} release. The same experiment was performed with extracellular stimulation using voltage pulses at an amplitude that can elicit the contraction of the isolated cells without EGTA-AM. To get better calcium imaging without contraction of the cells, we added low levels of EGTA-AM (50–200 µM) following Kornyeyev et al. (2010). Cells being stimulated for transilluminated overlayed and just fluorescence images are shown in Fig. 6c for control and LTB 0.2 µg/ml. The Ca^{2+} oscillations over time were plotted and are shown in Fig. 6d. At variance with the control, upon stimulation higher levels of the local events were observed for the same pulses (see arrows and peaks in Fig. 6d). As it happened without extracellular stimulation, the amplitudes and variability of Ca^{2+} oscillations after the addition of 0.2 µg/ml LTB were also increased. As expected, the average basal levels of Ca^{2+} and fluorescent signals upon stimulation are both increased by applying the same extracellular stimulation. This experiment showed that LTB promotes the dysregulation of Ca^{2+}

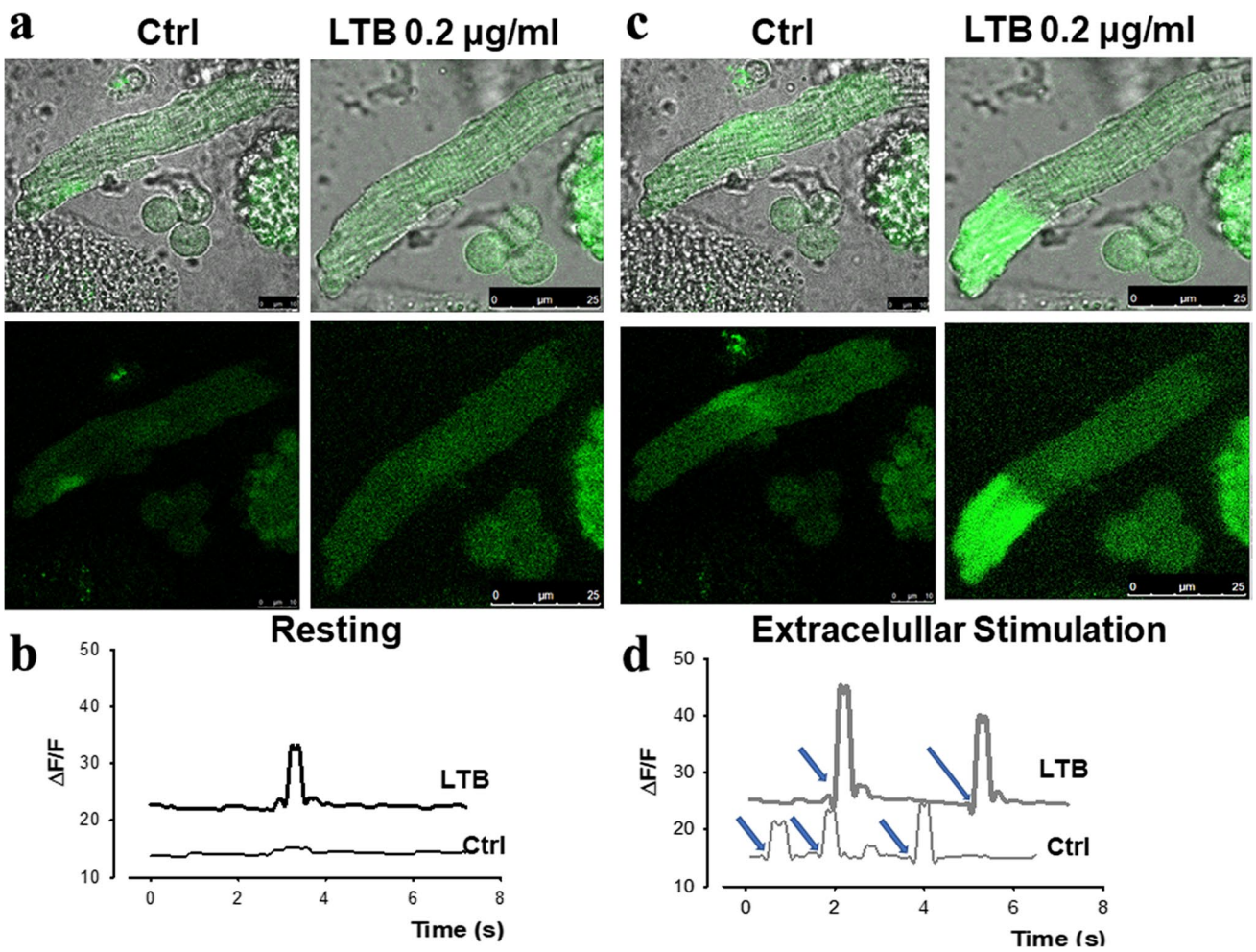

Fig. 6 LTB effects on basal global Ca^{2+} and intracellular Ca^{2+} release events in resting and extracellularly stimulated ventricular cardiomyocytes. **a** Images of resting non-stimulated cardiomyocytes in control culture and after 5 min of acute exposure to 0.2 µg/ml LTB (*right panel*). The images above correspond to the overlayed transilluminated images in both conditions. Below are the corresponding images only with the Fluo-3AM fluorescence. The green fluorescence in the isolated cardiomyocyte represents intracellular Ca^{2+}. **b** Recordings of global Ca^{2+} signals measured as $\Delta F/F$ from Fluo-3AM cell images versus time in control (*thin trace*) and LTB toxin-treated (*thick trace*) non-stimulated myocytes. The acute exposure of the myocytes to 0.2 µg/ml LTB toxin increased the basal fluorescence of the dye bound to intracellular Ca^{2+} after 5 min. In LTB, intracellular Ca^{2+} spontaneous oscillations appeared between 23 and 33 $\Delta F/F$ (fluorescence per background fluorescence ratio). Moreover, at rest, the variability between the amplitude of the oscillations was larger in the LBT-treated than in the control cells (14.29 ± 0.39 compared with 22.93 ± 2). A *t*-test comparing the measurements of Fluo-3AM in the same cells, for 72 different frames in control and LTB, showed that the difference in the mean values between the two groups is greater than would be expected by chance, with a statistically significant difference (n=3, p<0.001). The local Ca^{2+} release events seemed to be larger in the presence of LTB than in control, suggesting dysregulation of intracellular Ca^{2+}. **c** Images of cardiomyocytes after extracellular stimulation pulses in control (*left panel*) and after 5 min exposure to 0.2 µg/ml LTB (*right panel*). The images above are transilluminated overlayed images with fluorescent signals. The images below correspond to the fluorescence channel for calcium signaling. **d** Plot of the relative fluorescence intensity of Fluo-3AM bound to calcium versus time from the images shown in **c**. Plots are from global Ca^{2+} signals from the isolated cells in control (*thin trace*) and LTB toxin-treated stimulated myocytes (*thick traces*). After 5 min in 0.2 µg/ml LTB and extracellular stimulation, the myocytes showed a significant increase in both the basal fluorescence of Fluo-3AM bound to intracellular Ca^{2+} and the intensity of intracellular local Ca^{2+} release events upon stimulation (see arrows). In the stimulated myocytes, the basal intracellular Ca^{2+} concentration and Ca^{2+} increment when pulses were applied are significantly increased by LTB. As it happened without extracellular stimulation, the amplitudes and variability of Ca^{2+} oscillations after the addition of 0.2 µg/ml LTB were also increased (16.5 ± 2.68 compared with 26.5 ± 4.7). A *t*-test comparing the measurements of Fluo-3AM in the same stimulated cells, for 72 different frames in control and LTB, showed that the difference in the mean values between the two groups is greater than would be expected by chance, having a statistically significant difference (n=3, p = <0.001). Both basal values (control and LTB) are also increased in stimulated myocytes in comparison with cardiomyocytes in the resting state

homeostasis either in non-stimulated or stimulated cells, and this is more severe in situations where the functional reserve of the cardiac myocytes has been compromised (using extracellular stimulation compared to no stimulation). Thus, LTB promotes not only alterations in the pattern of excitability of cardiac myocytes but also their intracellular Ca^{2+} homeostasis. This latter finding is consistent with previous results here where LTB altered the pattern of contraction in isolated hearts, releasing more than the usual Ca^{2+} in the first contraction and releasing less Ca^{2+} in the second contraction. In summary, LTB promoted an incremental change in intracellular Ca^{2+} concentration. Extracellular stimulation of the cardiac myocytes promoted a faster and additional increment of intracellular Ca^{2+} concentration that remained high in between successive alternans pulses.

Intracellular Ca^{2+} is often altered in the pathogenic mechanisms of bacterial toxins. Whereas some bacteria can produce toxins that compromise cell membrane integrity or permeability leading to Ca^{2+} fluxes (Bouillot et al. 2018), others have evolved factors termed effectors that can either promote or inhibit Ca^{2+} fluxes in the absence of membrane permeabilization, usually requiring multiprotein complexes for their effect in Ca^{2+} fluxes in the cells (Wanford and Odendall 2023). In the case of bacterial pore-forming toxins, those changes can be fast and quite dramatic, leading eventually to cell death (Bouillot et al. 2018). Cells have developed during evolution protection mechanisms characterized by membrane repair and Ca^{2+} efflux mechanisms in order to survive these changes (Babiychuk and Draeger 2015; Cooper and McNeil 2015). PTFs can promote Ca^{2+} influx directly within the phagosome formed in the cell membrane (Shaughnessy et al. 2006) or through Ca^{2+} induced Ca^{2+} release from organelles enriched in Ca^{2+}, like the endoplasmic reticulum or the lysosomes (Krause et al. 1998), or through activation of Ca^{2+} permeable channels from the membrane (Staali et al. 1998). The Ca^{2+} influx through PTFs usually is massive and displays a monophasic kinetics, but multiphasic kinetics can be observed in the process of cell repair mechanisms or the progression of the cells towards death (Bouillot et al. 2018). However, though they are less frequent, Ca^{2+} oscillations, similar to the ones described in this section, have also been reported, for example, for streptolysin O (SLO) from *Streptococcus pyogenes* and hemolysin from *Staphylococcus aureus* which induce the release of Ca2+ from the endoplasmic reticulum activating inositol triphosphate receptors (IP3 receptors), having transient Ca^{2+} oscillations in the cells (Krause et al. 1998).

Many Gram-negative enteropathogens, like *Shigella flexneri* (producing hundreds of millions of cases of dysenteria worldwide (Musher and Musher 2004), produces alterations of intracellular Ca^{2+} through effectors. Effector proteins are injected into the host cytosol-enhancing Ca^{2+} transients that involve the IP3 receptors, eliciting Ca^{2+} oscillations (Konradt et al. 2011; Tran Van Nhieu et al. 2013; TranVan Nhieu et al. 2004). The enteropathogenic (EPEC) *E. coli* strain also behaves in a similar way, promoting Ca^{2+} oscillations in the host cells through effectors (Zhong et al. 2020). In neurons, it has been shown that the B subunit of the cholera toxin bound to the GM1 receptor increases intracellular Ca^{2+} (Milani et al. 1992). GM1 activation by the B subunit seems to be important to have a trophic effect in cerebellar granular neurons, promoting these Ca^{2+} oscillations (Wu et al. 1996). An increase in Ca^{2+} oscillations using the B subunit of the cholera toxin has been reported when the toxin is bound to GM1 in human Jurkat T-cell lines (Gouy et al. 1994). The modulation of Ca^{2+} signaling seems to be tightly related to the oligo-saccharide portion of the GM1 receptor (Lunghi et al. 2020). Interestingly, an augmentation of Ca^{2+} influx has also been reported for the heat-stable enterotoxin in the intestine (Dreyfus et al. 1993). Work performed in the 1980s suggested that the heat-labile enterototoxin (LTB) from *E. coli* also increases intracellular Ca^{2+}, interfering with the Ca^{2+}-calmodulin pathway (Goyal et al. 1989). The GM1 ganglioside modulates the Ca^{2+}-calmodulin pathway (Benfenati et al. 1991). Actually, calmodulin is a ganglioside-binding protein, whose binding properties can be altered by the presence of Ca^{2+} or molecules bound to the gangliosides (Higashi et al. 1992). It has recently been shown that Ca2+-calmodulin-dependent inactivation of Ryr2 may explain Ca2+ alternans in intact heart (Wei et al. 2021). The results obtained with the B subunit of the cholera toxin which is highly similar to LTB from *E. coli*, in Ca^{2+} transients and Ca^{2+} oscillations from several cells, are completely consistent with the results reported here.

A possible interpretation of the results from molecular dynamics to virtual heart simulations

A molecular dynamics simulation of the GM1 ganglioside bound to LTB was made to understand the biophysical changes promoted by LTB that could help understand the various effects observed in ion channels (Fig. 7). The crystal structure of LTB protein was obtained using PDB 1PZI (Mitchell et al. 2004), which was embedded in a (1-palmitoyl-2-oleoyl-sn-glycero-3-phosphocholine) (POPC) membrane containing 30% GM1 with a KCl concentration of 0.15 M by using the CHARMM-GUI software (Jo et al. 2008; Lee et al. 2016) and the charmm36 force field for lipid (Klauda et al. 2010), protein, and carbohydrates (Guvench et al. 2008). Molecular dynamics simulation was employed with the AMBER18 software (Case et al. 2018), under NTV conditions for a duration of 1000 ns. Temperature control was maintained using the Langevin thermostat (Hünenberger 2005). Non-bonded interactions were truncated at 10 Å, and long-range electrostatics were handled using the particle-mesh Ewald

(PME) under periodic boundary conditions (PBC) (Essmann et al. 1995). Additionally, we applied the SHAKE protocol (Ryckeart et al. 1977) to hydrogen atom bonding and the hydrogen mass-repartition to use an integration time step of 4 fs (Gao et al. 2021). The analysis of the simulation results was performed using an AMBERTOOLS program (Case et al. 2018). The initial structure of the LTB protein embedded in a membrane POPC containing 30% is presented in Fig. 7a. Figure 7b shows that the main interaction with GM1 occurs mostly in three LTB protomers, being quite similar to what it has been reported for the *Cholera Toxin* (Basu and Mukhopadhyay 2014). In Fig. 7c, the electron density profile of each membrane component is shown alone, revealing a proximal thickening of the membrane of 0.4 nm with POPC and that GM1 is a particular component of the membrane whose density profile complements the POPC inner left. This analysis works as a control showing that the model is suitable as a representation for both POPC membranes and GM1 gangliosides, alone or together. Lipid order parameters such as sn1 (measuring the correlation of the lipid tails in PC from POPC, closer to 1 implying higher order) are represented in Fig. 7d. The lipid parameter sn-2 (measures the correlation of the lipids of PO in POPC) is shown in Fig. 7e. Figures 7 d and e show that near GM1, lipids gain order and that they likely become less fluent. The lipid tails within an 8 Å sphere of LTB exhibit increased order parameters. This is crucial for understanding the physical properties of the membrane in the presence GM1, and this might change with toxin binding, as it usually happens. Finally, we have also analyzed the density profile of K^+ that is incremented in the region where GM1 and the toxin are present. This is not a specific binding for K^+, and it might occur probably for all cations because of this reason. This is shown in Supp. Fig. 4. This result shows that the GM1-LTB binding could have a screening effect related to the membrane potential of the surrounding molecules nearby. These results show that the binding of LTB alters the biophysical properties and organization of the membrane. This is consistent with previous studies that have shown that ganglioside GM1 can enhance the function of multiple proteins, including PKC, by modifying the biophysical properties of the membrane (Pei et al. 2002) or voltage-dependent Ca^{2+} channels (Carlson et al. 1994; Lunghi et al. 2020; Marengo et al. 1998), by accumulating positive ions on the outer membrane. To summarize, Fig. 7 illustrates with molecular dynamics simulations and analysis, that the binding of LTB to GM1 on the membrane, in addition to activation of the PTK and Extracellular Signal-Regulated Kinase (*Erk*) pathways (Duchemin et al. 2002), can also modify the lipid bilayer physicochemical properties, potentially leading to the changes described previously (including changes in the the Ca^{2+}-calmodulin pathway with calmodulin linked to GM1), leading to the observed cardiac alternans pattern that may lead to arrhythmogenesis and sudden cardiac death (Costantini et al. 2000; Wilson et al. 2009; Wilson and Rosenbaum 2007).

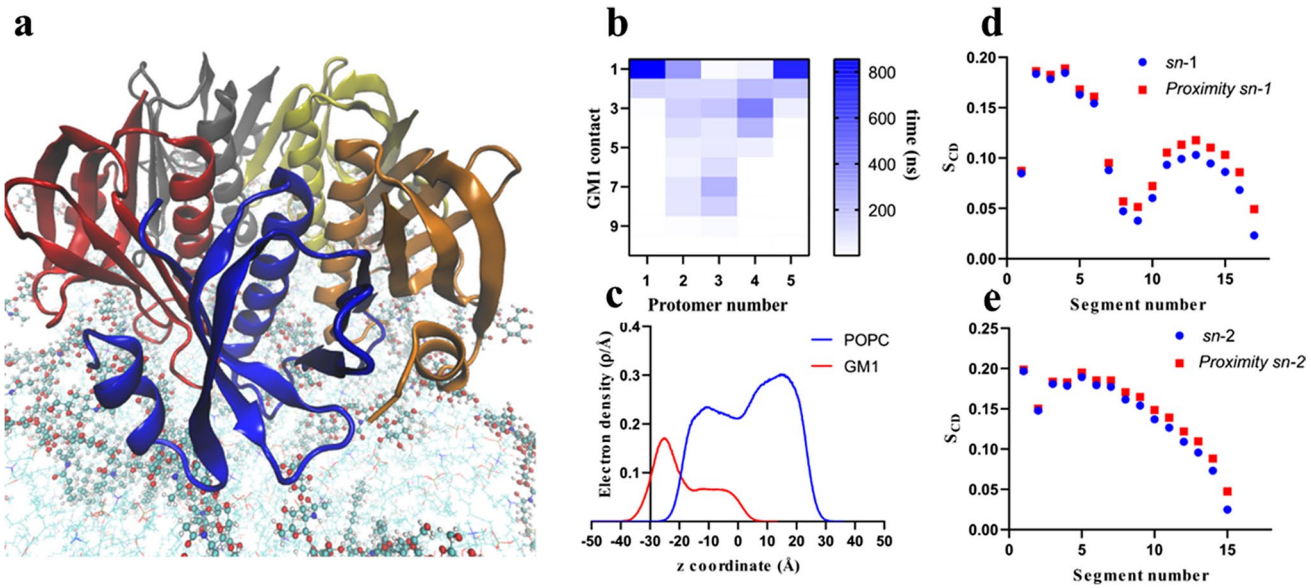

Fig. 7 Structural and biophysical analysis of GM1-LTB protein binding with the membrane using computational analysis. **a** The initial structure of the LTB protein embedded in a POPC membrane containing 30% GM1. **b** Healing map of the Interaction between LTB protomers and GM1 along the simulation time. **c** Electron density profile of each membrane component. **d** Lipid order parameters of sn-1 and **e** lipid order parameters of sn-2

A general scheme and simulation of the results with a virtual heart model using a modified model of the LabHeart model (Puglisi and Bers 2001) are summarized in Fig. 8. The figure explains the main results obtained in this report regarding the mechanism of action of LTB in the heart. LTB-GM1 binding increases the release of Ca^{2+} through RyR 2, resulting in the first peak of contraction in a mechanical alternans cycle (thick arrow from RyR 2 in Fig. 8). The Ca^{2+} release through RyR 2 is less during the second contraction in a mechanical alternans cycle due to the presence of less Ca^{2+} inside the SR, as SERCA could not refill the SR with Ca^{2+} at levels like the first contraction (dash arrow from RyR 2 in Fig. 8). This interpretation is consistent with a recent report from the group of Dr. Escobar that states that SERCA plays a central role in generating alternans patterns of contraction in the heart (Millet et al. 2021; Short 2021). LTB binding also has consequences in terms of ion channel activity. The Na^+ channel is inhibited by LTB, while the slow K^+ delayed rectifier channels, hERG (IKr) and KCNQ (IKs), are mildly enhanced. The ICa currents through Cv1.2 inactivated and might not recover enough from inactivation for the 2nd AP. The Ca^{2+} release from the SR could also contribute to the inhibition of ICa through Ca^{2+}-dependent inactivation during the 2nd AP. All these effects may result in electrical alternans of the action potentials. The extra Ca^{2+} release from the SR during the first contraction of an alternans cycle or the leak of $Ca^{2+}$from the SR could impact the Na^+-Ca^{2+} exchanger (NCX) leading to cardiac dysfunction or another pro-arrhythmogenic effect of LTB, such as DAD (Bers 2014). The inset in Fig. 8 with red solid lines is a simulation obtained with a modified version of LabHeart (Puglisi and Bers 2001). The simulation shows in thin lines the alternans pattern for AP, intracellular Ca^{2+}, and tension. All the experimental results reported here have been introduced in LabHeart, being the only difference between the 1st and 2nd AP, the inactivation of ICa produced by the toxin and enhanced release by RyR 2, and a minor change towards less Ca^{2+} release and less Ca^{2+} uptake by the SR. The main

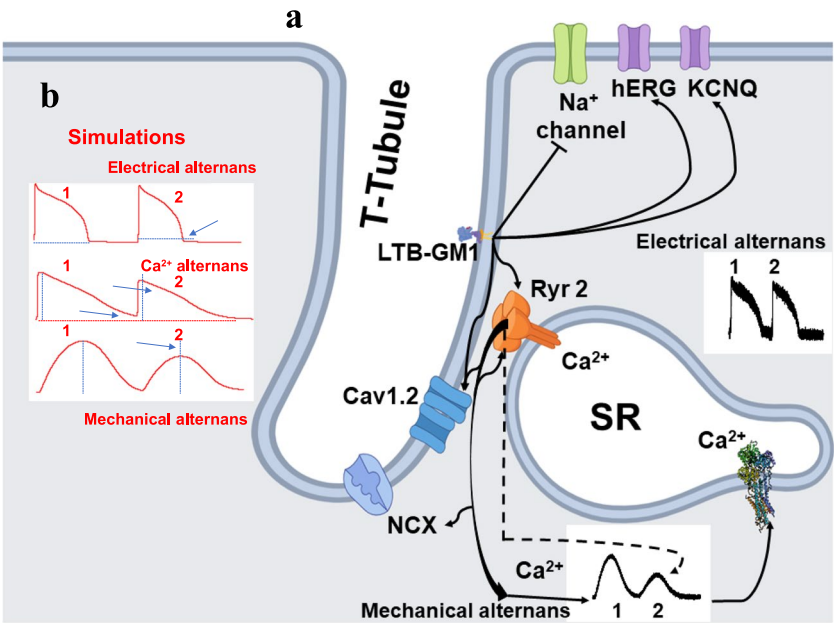

Fig. 8 Summary of the effects of LTB-GM1 binding on heart cells. **a** The mechanical alternans are caused by enhancing Ca^{2+} release through the first contraction during an alternans cycle. However, it is crucial to explain our observations that the refill of Ca^{2+} by SERCA is not enough to get a strong second Ca^{2+} release for the second contraction. Overall, this leads to Ca^{2+} homeostasis dysregulation. The electrical alternans might be caused by the multiple effects on Na^+, K^+, and Ca^{2+} (Cav1.2) channels (created with BioRender.com). The LTB-GM1 binding will impact in all the membranes from the cardiomyocyte in particular microdomains or lipid rafts. **b** Simulation of action potentials, calcium, and tension alternans in two consecutive beats, obtained using a modified version of Labheart. The main experimental features were reproduced assuming the effects observed on ICa, INa, IK (hERG), and only a mild increase in the release by RyR 2 channels. The uptake was slightly diminished. The simulated traces are all in red. The *upper traces* correspond to electrical alternans. The dashed blue line represents the duration of the AP at the first beat. For comparison, it was copied in the second beat. The arrow indicates the difference observed. The *middle traces* correspond to Ca^{2+} alternans. The red dashed line indicates the zero level of Ca^{2+}. Note that after the first beat, Ca^{2+} levels do not return to zero (indicated by the blue arrow between traces). This might condition Ca^{2+} reuptake by SERCA affecting the Ca^{2+} pool inside the SR to be released during the 2nd beat. The dashed vertical blue line indicates the height of the Ca^{2+} transient during the first beat. Note that there is a significant reduction of the release during the 2nd beat. The *bottom traces* represent the mechanical alternans. The dashed vertical blue line represents the height of the amplitude of tension during the first beat. For comparison, it was placed in the second beat, and the arrow indicated that the height in this condition is significantly lower getting a mechanical alternans

experimental features reproduced by the simulation with these assumptions are indicated in the figure.

Further research will be needed to elucidate the precise molecular mechanism by which the toxin promotes cardiac alternans.

Concluding remarks

In this letter, we have shown that many bacterial toxins can have detrimental effects on the heart. From those that act on the membrane, we have shown that both pore-forming toxins (PFTs) and toxins that exert their effects through membrane receptors may change heart function altering membrane permeability and excitability, leading to Ca2+ influx and a loss of Ca2+ homeostasis, critical for normal heart functioning. Usually, PFTs' effects in the heart are more dramatic and have been also more characterized and well-established for multiple toxins and multiple bacteria. Related to toxins binding to membrane receptors, because of their greater diversity, less is known. However, there is intriguing information related to the close statistical association between heat-labile enterotoxin (LTB) from children infected with ETEC *E. coli* and sudden cardiac death in those (Bettelheim et al. 1989; Morris et al. 2009; Murrell et al. 1993). LTB binds to GM1 gangliosides that are abundant in the heart. We tested the effects of LTB on isolated hearts and cardiomyocytes to know if, in the scope of this letter, this could be a plausible explanation for the statistical association mentioned above.

The results we obtained have several implications: (i) The binding of LTB to its presumed receptor GM1 resulted in profound alterations in heart and cardiac cell function promoting disturbances in the form of alternans. This occurred even at very low doses of LTB. In several cell types, GM1 ganglioside responses caused by ligand binding are closely linked to intracellular Ca^{2+} concentrations, localizations, and their variabilities (Ledeen and Wu 2002). Since most gangliosides are localized at the plasma membrane in lipid rafts (Blank et al. 2007), the B subunits from AB_5 toxins can be used to bind specifically to these gangliosides, and such binding and subsequent events can be used to study the effects of B-subunit toxins on cells (Beddoe et al. 2010). As a model for this process, we used ventricular cardiomyocytes, which have plasma membrane lipid rafts with ample numbers (Bers and Morotti 2014) of GM1 receptors (Maguy et al. 2006). It has been reported that ventricular cardiomyocytes can be altered in their cellular properties by the binding of LTB (Montpetit et al. 2009). Our results with ex vivo guinea pig hearts also confirmed that the binding of LTB caused changes in surface electrograms and tensions. The altered patterns of electrical and tension recordings appeared at LTB concentrations near the IC50 for cholera toxin B subunit-GM1 binding. In summary, we found that LTB binding to GM1 receptors in cardiomyocytes was correlated with mechanical and electrical alternans. In particular, because of alternans, they can be related to rate changes in the molecules critical for Ca^{2+} dynamics and release/uptake from intracellular stores (Wilson et al. 2006).

The possibility that infections by some *E. coli* strains resulting in the delivery of enterotoxins into the blood circulation can affect cardiac function should be considered based on our results. Elsewhere, it has been shown that discordant alternans are a manifestation of sudden cardiac death in animal models and clinical trials (Kim et al. 2014; Verrier and Nearing 1994). In our experiments, we observed a pattern of alternans at low doses of extracellular LTB up to its IC50. Increasing concentrations of LTB promoted a change in the electrical and tension patterns, which could yield ventricular fibrillation in vivo (Hastings et al. 2000; Skardal and Restrepo 2014). Ventricular fibrillation is a common manifestation in sudden cardiac death syndromes (Israel 2014). The results presented here support the notion reported previously that cardiac function is impaired by enterotoxins and that this could result in sudden cardiac death (Bettelheim et al. 1990). This issue might be particularly relevant for sudden cardiac death in infants, where the causes of demise have not yet been established (Panicker et al. 2012). Our results support the hypothesis that at least a fraction of these lethal cases might be due to bacterial infections and the coronary alterations reported here.

Do LBT toxins from enterotoxigenic bacteria play a role in sudden cardiac death? Here, we found that the results using ex vivo hearts compared to isolated heart cells were consistent. In vivo, patients may have diarrhea with different levels of toxins in the blood. The passage of the toxins to the blood is related to the transport and damage of toxins by intestinal epithelial cells. The results point to a critical role for ganglioside signaling in keeping the correct homeostasis of cardiac cells through the modulation of intracellular Ca^{2+} dynamics. The binding of LTB to GM1 ganglioside receptors and subsequent intracellular events disrupted this precise control, generating alterations in Ca^{2+} release and uptake promoting alternans contractions. The findings reported in this paper may be of relevance to the mechanism of sudden cardiac death where a critical role of alternans in the process of cardiac failure has been established (Rubenstein and Lipsius 1995; Sarusi et al. 2014). Sudden infant cardiac death or sudden infant death syndrome (SIDS) is a worldwide problem whose causes have remained elusive. Several events have been proposed as playing a role in SIDS. For example, it has been known for some time that enterotoxigenic strains of *E. coli* have been found in the intestines of children with SIDS (Bettelheim et al. 1990; Siarakas et al. 1999). Moreover, a connection between bacteremia and cardiac arrhythmias has also been proposed (Morris

et al. 2009). The results presented here are consistent with the hypothesis of Bettelheim et al., that a fraction of SIDS is due to toxins released from bacteria (Bettelheim and Goldwater 2015; Bettelheim et al. 1990; Morris et al. 2009). From our results, we propose an elaboration of this mechanism that could explain why enterotoxin B-subunits can lead to SIDS. However, we cannot rule out other causes as additional contributing factors to SIDS. Further experiments are needed to clarify to which extent ETEC is a cause of SIDS and more details regarding the molecular interactions involved in the mechanisms reported here.

In summary, we have shown that bacterial toxins can have a profound impact on heart function, and we have presented evidence of a new mechanism of cardiac damage that could lead to arrhythmias and sudden cardiac death, promoted by another bacterial toxin, explaining epidemiological findings found by several groups. The binding of B-subunits of LTB to cardiac cell surface gangliosides can lead to alterations of cellular functions that can have repercussions to the entire heart leading to arrhythmogenesis and sudden cardiac death. Among the effects of LTB were alterations in the activities of ion channels and a pattern of alternans contractions. Thus, our results may ultimately help to explain the contributions of ETEC to SIDS.

Supplementary Information The online version contains supplementary material available at https://doi.org/10.1007/s12551-023-01100-6.

Acknowledgements GF wants to acknowledge the support from Universidad de la República and particularly from CSIC UdelaR, SNI ANII, and PEDECIBA, Uruguay. Also, the personnel at the animal facility, accountant, personnel dean office, and buying departments at the School of Medicine, UdelaR, Uruguay, are acknowledged for their support. Maribel Monzon is acknowledged for her support during all the stages of this work.

Author contribution Conceptualization: Gonzalo Ferreira.
Funding acquisition: Gonzalo Ferreira.
Supervision: Gonzalo Ferreira.
Methodology: Gonzalo Ferreira.
Visualization: Gonzalo Ferreira, José Puglisi, Garth L. Nicolson, Romina Cardozo, and Carlos Costa.
Software: Gonzalo Ferreira, José Puglisi, Carlos Costa, Santiago Sastre, Romina Cardozo, Axel Santander, and Luisina Chavarría.
Investigation and validation: Gonzalo Ferreira, Santiago Sastre, Carlos Costa, Romina Cardozo, Axel Santander, and Garth Nicolson.
Data curation: Gonzalo Ferreira, Romina Cardozo, Carlos Costa, and Santiago Sastre.
Resources (samples/reagents): Gonzalo Ferreira.
Formal analysis: Gonzalo Ferreira, Carlos Costa, Santiago Sastre, Valentina Guizzo, Romina Cardozo, Axel Santander, and Luisina Chavarría.
Project administration: Gonzalo Ferreira and Romina Cardozo.
Writing—original draft: Gonzalo Ferreira, Garth L. Nicolson, and Santiago Sastre.
Writing—editing and reviewing: Gonzalo Ferreira, Garth L. Nicolson, Santiago Sastre, Romina Cardozo, Axel Santander, and Luisina Chavarría.
Gonzalo Ferreira wrote the scientific project, performed the experiments, analyzed the data, and wrote the draft manuscript and later versions with feedback from all authors, especially Romina Cardozo and Santiago Sastre. Garth Nicolson and José Puglisi edited the manuscript and discussed the results with Gonzalo Ferreira. Gonzalo Ferreira, Romina Cardozo, and Carlos Costa performed most of the experiments and analyzed the data (including material preparation, data collection, and analysis). Carlos Costa had a minor role in writing the manuscript. Santiago Sastre helped in writing the discussion and performing the molecular dynamics simulation. Romina Cardozo, Axel Santander, Valentina Guizzo, and Luisina Chavarría performed some experiments (including material preparation, data collection, and analysis) and helped prepare the manuscript. All authors read and approved the final manuscript.

Funding This study was funded by CSIC-Universidad de la República (UdelaR) (Uruguayan national funds) (grant proposals p941, p146, p91, p137, p22520220100007UD 2022) and by PDT 7643 (Interamerican Bank of Development funds) to Gonzalo Ferreira (GF). G.F. is also grateful to the CSIC human resources for the International Cooperation Program (MIA), SNI-ANII, and PEDECIBA. GF is also thankful for the encouragement to ANII (Uruguay) and PAIE CSIC. Garth Nicolson is supported by the Institute for Molecular Medicine, USA.

Data availability All relevant data are within the paper or supplemental figures.

Declarations

Ethical approval All applicable international, national, and/or institutional guidelines for the care and use of animals were followed according to bio-ethical procedures accepted by the American Association for Laboratory Animal Sciences (IACUC).

All animal studies have been approved by the appropriate ethics committee and have therefore been performed in agreement with the ethical standards laid down in the 1964 Declaration of Helsinki and its later amendments. Guidelines for ethics approval according to specific national laws were revised by the Honorary Committee of Animal Experimentation (CHEA), from Uruguay. Animal ethics and experimentation protocols were examined to pursue the international guidelines on animal experimentation mentioned above (approval protocol number 071140-000467-09, CHEA). No anesthesia was used to avoid interferences with the heart function. To euthanize the animals, instantaneous occipital concussion was used.

Consent to participate All authors have declared their consent to participate.

Consent for publication All the authors have declared their consent to publish.

Conflict of interest The authors declare no competing interests.

References

Abrams ST, Wang L, Yong J, Yu Q, Du M, Alhamdi Y, . . . Wang G (2022) The importance of pore-forming toxins in multiple organ injury and dysfunction. Biomedicines 10(12). https://doi.org/10.3390/biomedicines10123256

Ahern CA, Zhang JF, Wookalis MJ, Horn R (2005) Modulation of the cardiac sodium channel NaV1.5 by Fyn, a Src family tyrosine kinase. Circ Res 96(9):991–998. https://doi.org/10.1161/01.RES.0000166324.00524.dd

Alhamdi Y, Neill DR, Abrams ST, Malak HA, Yahya R, Barrett-Jolley R, . . . Toh CH (2015) Circulating pneumolysin is a potent inducer of cardiac injury during pneumococcal infection. PLoS Pathog 11(5):e1004836. https://doi.org/10.1371/journal.ppat.1004836

Alvarez-Lacalle E, Cantalapiedra IR, Penaranda A, Cinca J, Hove-Madsen L, Echebarria B (2013) Dependency of calcium alternans on ryanodine receptor refractoriness. PLoS One 8(2):e55042. https://doi.org/10.1371/journal.pone.0055042

Anderson R, Nel JG, Feldman C (2018) Multifaceted role of pneumolysin in the pathogenesis of myocardial injury in community-acquired pneumonia. Int J Mol Sci 19(4). https://doi.org/10.3390/ijms19041147

Antoniou CK, Dilaveris P, Manolakou P, Galanakos S, Magkas N, Gatzoulis K, Tousoulis D (2017) QT prolongation and malignant arrhythmia: how serious a problem? Eur Cardiol 12(2):112–120. https://doi.org/10.15420/ecr.2017:16:1

Ashpole NM, Herren AW, Ginsburg KS, Brogan JD, Johnson DE, Cummins TR, . . . Hudmon A (2012) Ca2+/calmodulin-dependent protein kinase II (CaMKII) regulates cardiac sodium channel NaV1.5 gating by multiple phosphorylation sites. J Biol Chem 287(24):19856-19869. https://doi.org/10.1074/jbc.M111.322537

Babiychuk EB, Draeger A (2015) Defying death: cellular survival strategies following plasmalemmal injury by bacterial toxins. Semin Cell Dev Biol 45:39–47. https://doi.org/10.1016/j.semcdb.2015.10.016

Balijepalli RC, Delisle BP, Balijepalli SY, Foell JD, Slind JK, Kamp TJ, January CT (2007) Kv11.1 (ERG1) K+ channels localize in cholesterol and sphingolipid enriched membranes and are modulated by membrane cholesterol. Channels (Austin) 1(4):263–272. https://doi.org/10.4161/chan.4946

Balijepalli RC, Kamp TJ (2008) Caveolae, ion channels and cardiac arrhythmias. Prog Biophys Mol Biol 98(2-3):149–160. https://doi.org/10.1016/j.pbiomolbio.2009.01.012

Balshaw D, Gao L, Meissner G (1999) Luminal loop of the ryanodine receptor: a pore-forming segment? Proc Natl Acad Sci 96(7):3345–3347. https://doi.org/10.1073/pnas.96.7.3345

Basu I, Mukhopadhyay C (2014) Insights into binding of cholera toxin to GM1 containing membrane. Langmuir 30(50):15244–15252. https://doi.org/10.1021/la5036618

Beddoe T, Paton AW, Le Nours J, Rossjohn J, Paton JC (2010) Structure, biological functions and applications of the AB5 toxins. Trends Biochem Sci 35(7):411–418. https://doi.org/10.1016/j.tibs.2010.02.003

Benfenati F, Fuxe K, Agnati LF (1991) Ganglioside GM1 modulation of calcium/calmodulin-dependent protein kinase II activity and autophosphorylation. Neurochem Int 19(3):271–279. https://doi.org/10.1016/0197-0186(91)90011-2

Bers DM (2014) Cardiac sarcoplasmic reticulum calcium leak: basis and roles in cardiac dysfunction. Annu Rev Physiol 76:107–127. https://doi.org/10.1146/annurev-physiol-020911-153308

Bers DM, Morotti S (2014) Ca(2+) current facilitation is CaMKII-dependent and has arrhythmogenic consequences. Front Pharmacol 5:144. https://doi.org/10.3389/fphar.2014.00144

Bers DM, Peskoff A (1991) Diffusion around a cardiac calcium channel and the role of surface bound calcium. Biophys J 59(3):703–721. https://doi.org/10.1016/s0006-3495(91)82284-6

Bettelheim KA, Dwyer BW, Smith DL, Goldwater PN, Bourne AJ (1989) Toxigenic Escherichia coli associated with sudden infant death syndrome. Med J Aust 151(9):538. https://doi.org/10.5694/j.1326-5377.1989.tb128512.x

Bettelheim KA, Goldwater PN (2015) Escherichia coli and sudden infant death syndrome. Front Immunol 6:343. https://doi.org/10.3389/fimmu.2015.00343

Bettelheim KA, Goldwater PN, Dwyer BW, Bourne AJ, Smith DL (1990) Toxigenic Escherichia coli associated with sudden infant death syndrome. Scand J Infect Dis 22(4):467–476 Retrieved from http://www.ncbi.nlm.nih.gov/pubmed/2218409

Blackwell CC, Gordon AE, James VS, MacKenzie DA, Mogensen-Buchanan M, El Ahmer OR, . . . Busuttil A (2002) The role of bacterial toxins in sudden infant death syndrome (SIDS). Int J Med Microbiol 291(6-7):561-570. Retrieved from http://www.ncbi.nlm.nih.gov/pubmed/11892683

Blank N, Schiller M, Krienke S, Wabnitz G, Ho AD, Lorenz HM (2007) Cholera toxin binds to lipid rafts but has a limited specificity for ganglioside GM1. Immunol Cell Biol 85(5):378–382. https://doi.org/10.1038/sj.icb.7100045

Blauwet LA, Cooper LT (2010) Myocarditis. Prog Cardiovasc Dis 52(4):274–288. https://doi.org/10.1016/j.pcad.2009.11.006

Bolz DD, Li Z, McIndoo ER, Tweten RK, Bryant AE, Stevens DL (2015) Cardiac myocyte dysfunction induced by streptolysin O is membrane pore and calcium dependent. Shock 43(2):178–184. https://doi.org/10.1097/shk.0000000000000266

Bouillot S, Reboud E, Huber P (2018) Functional consequences of calcium influx promoted by bacterial pore-forming toxins. Toxins (Basel) 10(10). https://doi.org/10.3390/toxins10100387

Boulnois GJ, Paton JC, Mitchell TJ, Andrew PW (1991) Structure and function of pneumolysin, the multifunctional, thiol-activated toxin of Streptococcus pneumoniae. Mol Microbiol 5(11):2611–2616. https://doi.org/10.1111/j.1365-2958.1991.tb01969.x

Bremer EG, Hakomori S (1984) Gangliosides as receptor modulators. Adv Exp Med Biol 174:381–394 Retrieved from http://www.ncbi.nlm.nih.gov/pubmed/6331135

Bremer EG, Hakomori S, Bowen-Pope DF, Raines E, Ross R (1984) Ganglioside-mediated modulation of cell growth, growth factor binding, and receptor phosphorylation. J Biol Chem 259(11):6818–6825 Retrieved from http://www.ncbi.nlm.nih.gov/pubmed/6327695

Busselberg D, Evans ML, Carpenter DO, Rahmann H (1989) Effects of exogenous ganglioside and cholesterol application on excitability of Aplysia neurons. Membr Biochem 8(1):19–26 Retrieved from http://www.ncbi.nlm.nih.gov/pubmed/2811702

Carlson RO, Masco D, Brooker G, Spiegel S (1994) Endogenous ganglioside GM1 modulates L-type calcium channel activity in N18 neuroblastoma cells. J Neurosci 14(4):2272–2281 Retrieved from http://www.ncbi.nlm.nih.gov/pubmed/7512636

Carmeliet E (1987) Voltage-dependent block by tetrodotoxin of the sodium channel in rabbit cardiac Purkinje fibers. Biophys J 51(1):109–114. https://doi.org/10.1016/s0006-3495(87)83315-5

Case DA, Ben-Shalom IY, Brozell SR, Cerutti DS, Cheatham TE, III, Cruzeiro VWD, Darden TA, DukeRE, Ghoreishi D, Gilson MK, Gohlke H, Goetz AW, Greene D, Harris R, Homeyer N, Huang Y, IzadiS, Kovalenko A, Kurtzman T, Lee TS, LeGrand S, Li P, Lin C, Liu J, Luchko T, Luo R, Mermelstein DJ, Merz KM, Miao Y, Monard G, Nguyen C, Nguyen H, Omelyan I, Onufriev A, Pan F, Qi R, Roe DR, Roitberg A, Sagui C, Schott-Verdugo S, Shen J, Simmerling CL, Smith J, Salomon-Ferrer R, Swails J, Walker RC, Wang J, Wei H, Wolf RM, Wu X, Xiao L, York DM, Kollman PA (2018) AMBER 2018, University of California, San Francisco. https://ambermd.org/doc12/Amber18.pdf

Chen X, Li HY, Hu XM, Zhang Y, Zhang SY (2019) Current understanding of gut microbiota alterations and related therapeutic intervention strategies in heart failure. Chin Med J (Engl) 132(15):1843–1855. https://doi.org/10.1097/cm9.0000000000000330

Cheng H, Lederer MR, Lederer WJ, Cannell MB (1996) Calcium sparks and [Ca2+]i waves in cardiac myocytes. Am J Physiol 270(1 Pt 1):C148–C159 Retrieved from http://www.ncbi.nlm.nih.gov/pubmed/8772440

Chun YS, Oh HG, Park MK, Cho H, Chung S (2013) Cholesterol regulates HERG K+ channel activation by increasing phospholipase C β1 expression. Channels (Austin) 7(4):275–287. https://doi.org/10.4161/chan.25122

Chun YS, Shin S, Kim Y, Cho H, Park MK, Kim TW, . . . Chung S (2010) Cholesterol modulates ion channels via

down-regulation of phosphatidylinositol 4,5-bisphosphate. J Neurochem 112(5):1286-1294. https://doi.org/10.1111/j.1471-4159.2009.06545.x

Cooper ST, McNeil PL (2015) Membrane repair: mechanisms and pathophysiology. Physiol Rev 95(4):1205–1240. https://doi.org/10.1152/physrev.00037.2014

Cortada E, Serradesanferm R, Brugada R, Verges M (2021) The voltage-gated sodium channel β2 subunit associates with lipid rafts by S-palmitoylation. J Cell Sci 134(6). https://doi.org/10.1242/jcs.252189

Costa C, Torres H, Hartmann H, Dutra J, Ferreira G (2014) Cardiomiopatías químicas: Repercusión funcional de la cloroquina en corazón aislado. Anales de la Facultad de Medicina 1(1):64–79. https://doi.org/10.25184/anfamed2014v1n1a1

Costantini O, Drabek C, Rosenbaum DS (2000) Can sudden cardiac death be predicted from the T wave of the ECG? A critical examination of T wave alternans and QT interval dispersion. Pacing Clin Electrophysiol 23(9):1407–1416 Retrieved from http://www.ncbi.nlm.nih.gov/pubmed/11025899

Dai Y, Luo W, Chang J (2018) Rho kinase signaling and cardiac physiology. Curr Opin Physiol 1:14–20. https://doi.org/10.1016/j.cophys.2017.07.005

Dal Peraro M, van der Goot FG (2016) Pore-forming toxins: ancient, but never really out of fashion. Nat Rev Microbiol 14(2):77–92. https://doi.org/10.1038/nrmicro.2015.3

Dallas WS, Falkow S (1980) Amino acid sequence homology between cholera toxin and Escherichia coli heat-labile toxin. Nature 288(5790):499–501. https://doi.org/10.1038/288499a0

Dawson RM (2005) Characterization of the binding of cholera toxin to ganglioside GM1 immobilized onto microtitre plates. J Appl Toxicol 25(1):30–38. https://doi.org/10.1002/jat.1015

Dixon SJ, Stewart D, Grinstein S, Spiegel S (1987) Transmembrane signaling by the B subunit of cholera toxin: increased cytoplasmic free calcium in rat lymphocytes. J Cell Biol 105(3):1153–1161 Retrieved from http://www.ncbi.nlm.nih.gov/pubmed/3654749

Dreyfus LA, Harville B, Howard DE, Shaban R, Beatty DM, Morris SJ (1993) Calcium influx mediated by the Escherichia coli heat-stable enterotoxin B (STB). Proc Natl Acad Sci U S A 90(8):3202–3206. https://doi.org/10.1073/pnas.90.8.3202

Duan Q, Xia P, Nandre R, Zhang W, Zhu G (2019) Review of newly identified functions associated with the heat-labile toxin of enterotoxigenic Escherichia coli. Front Cell Infect Microbiol 9(292). https://doi.org/10.3389/fcimb.2019.00292

Dubreuil JD, Isaacson RE, Schifferli DM (2016) Animal enterotoxigenic Escherichia coli. EcoSal Plus 7(1). https://doi.org/10.1128/ecosalplus.ESP-0006-2016

Duchemin AM, Ren Q, Mo L, Neff NH, Hadjiconstantinou M (2002) GM1 ganglioside induces phosphorylation and activation of Trk and Erk in brain. J Neurochem 81(4):696–707. https://doi.org/10.1046/j.1471-4159.2002.00831.x

DuMont AL, Torres VJ (2014) Cell targeting by the Staphylococcus aureus pore-forming toxins: it's not just about lipids. Trends Microbiol 22(1):21–27. https://doi.org/10.1016/j.tim.2013.10.004

Eidels L, Proia RL, Hart DA (1983) Membrane receptors for bacterial toxins. Microbiol Rev 47(4):596–620 Retrieved from http://www.ncbi.nlm.nih.gov/pubmed/6363900

Eisner DA, Caldwell JL, Kistamás K, Trafford AW (2017) Calcium and excitation-contraction coupling in the heart. Circ Res 121(2):181–195. https://doi.org/10.1161/circresaha.117.310230

Essmann U, Perera L, Berkowitz ML, Darden T, Lee H, Pedersen LG (1995) A smooth particle mesh Ewald method. J Chem Phys 103(19):8577–8593. https://doi.org/10.1063/1.470117

Euler DE (1999) Cardiac alternans: mechanisms and pathophysiological significance. Cardiovasc Res 42(3):583–590 Retrieved from http://www.ncbi.nlm.nih.gov/pubmed/10533597

Fan E, Merritt EA, Verlinde CL, Hol WG (2000) AB(5) toxins: structures and inhibitor design. Curr Opin Struct Biol 10(6):680–686 Retrieved from http://www.ncbi.nlm.nih.gov/pubmed/11114505

Ferreira de Mattos G, Costa C, Savio F, Alonso M, Nicolson GL (2017) Lead poisoning: acute exposure of the heart to lead ions promotes changes in cardiac function and Cav1.2 ion channels. Biophysical Reviews 9(5):807–825. https://doi.org/10.1007/s12551-017-0303-5

Ferreira G, Artigas P, De Armas R, Pizarro G, Brum G (1997a) Comparison of the effects of BDM on L-type Ca channels of cardiac and skeletal muscle. In: Sotelo JR, Benech JC (eds) Calcium and cellular metabolism. Springer, Boston, MA. https://doi.org/10.1007/978-1-4757-9555-4_5

Ferreira G, Artigas P, Pizarro G, Brum G (1997b) Butanedione monoxime promotes voltage-dependent inactivation of L-type calcium channels in heart. Effects on gating currents. J Mol Cell Cardiol 29(2):777–787 Retrieved from http://www.ncbi.nlm.nih.gov/pubmed/9140834

Ferreira G, Reyes N, Pizarro G, Brum G, Rios E (2001) Correlation between surfaces of inactivation of ionic currents and charge availability in L-type Ca2+ channels. Biophysical Society conference meeting book 2001.

Ferreira G, Rios E, Reyes N (2003) Two components of voltage-dependent inactivation in Ca(v)1.2 channels revealed by its gating currents. Biophys J 84(6):3662–3678. https://doi.org/10.1016/S0006-3495(03)75096-6

Ferreira G, Santander A, Chavarría L, Cardozo R, Savio F, Sobrevia L, Nicolson GL (2022) Functional consequences of lead and mercury exposomes in the heart. Mol Aspects Med 87:101048. https://doi.org/10.1016/j.mam.2021.101048

Ferreira G, Santander A, Savio F, Guirado M, Sobrevia L, Nicolson GL (2021) SARS-CoV-2, Zika viruses and mycoplasma: structure, pathogenesis and some treatment options in these emerging viral and bacterial infectious diseases. Biochim Biophys Acta Mol Basis Dis 1867(12):166264. https://doi.org/10.1016/j.bbadis.2021.166264

Fink M, Noble PJ, Noble D (2011) Ca^{2+}-induced delayed afterdepolarizations are triggered by dyadic subspace $Ca2^{2+}$ affirming that increasing SERCA reduces aftercontractions. Am J Physiol Heart Circ Physiol 301(3):H921–H935. https://doi.org/10.1152/ajpheart.01055.2010

Fishman PH, Pacuszka T, Orlandi PA (1993) Gangliosides as receptors for bacterial enterotoxins. Adv Lipid Res 25:165–187 Retrieved from http://www.ncbi.nlm.nih.gov/pubmed/8396312

Fleckenstein JM, Kuhlmann FM (2019) Enterotoxigenic Escherichia coli infections. Curr Infect Dis Rep 21(3):9. https://doi.org/10.1007/s11908-019-0665-x

Fossa AA, Wisialowski T, Wolfgang E, Wang E, Avery M, Raunig DL, Fermini B (2004) Differential effect of HERG blocking agents on cardiac electrical alternans in the guinea pig. Eur J Pharmacol 486(2):209–221. https://doi.org/10.1016/j.ejphar.2003.12.028

Fukunaga K, Miyamoto E, Soderling TR (1990) Regulation of Ca2+/calmodulin-dependent protein kinase II by brain gangliosides. J Neurochem 54(1):103–109. https://doi.org/10.1111/j.1471-4159.1990.tb13288.x

Gabellini N, Facci L, Milani D, Negro A, Callegaro L, Skaper SD, Leon A (1991) Differences in induction of c-fos transcription by cholera toxin-derived cyclic AMP and Ca2+ signals in astrocytes and 3T3 fibroblasts. Exp Cell Res 194(2):210–217 Retrieved from http://www.ncbi.nlm.nih.gov/pubmed/1851095

Gao Y, Lee J, Smith IPS, Lee H, Kim S, Qi Y, . . . Im W (2021) CHARMM-GUI supports hydrogen mass repartitioning and different protonation states of phosphates in lipopolysaccharides. J Chem Inf Model 61(2):831-839. https://doi.org/10.1021/acs.jcim.0c01360

Gill DM, Richardson SH (1980) Adenosine diphosphate-ribosylation of adenylate cyclase catalyzed by heat-labile enterotoxin of

Escherichia coli: comparison with cholera toxin. J Infect Dis 141(1):64–70 Retrieved from http://www.ncbi.nlm.nih.gov/pubmed/6988518

Glynn P, Musa H, Wu X, Unudurthi SD, Little S, Qian L, . . . Hund TJ (2015) Voltage-gated sodium channel phosphorylation at Ser571 regulates late current, arrhythmia, and cardiac function in vivo. Circulation 132(7):567-577. https://doi.org/10.1161/circulationaha.114.015218

Gouy H, Deterre P, Debre P, Bismuth G (1994) Cell calcium signaling via GM1 cell surface gangliosides in the human Jurkat T cell line. J Immunol 152(7):3271–3281 Retrieved from http://www.ncbi.nlm.nih.gov/pubmed/7511641

Goyal J, Ganguly NK, Garg UC, Walia BN (1989) Calcium calmodulin in altered NaCl transport by heat-labile enterotoxin of Escherichia coli. Biochem Int 18(6):1305–1314. https://pubmed.ncbi.nlm.nih.gov/2502117/

Grandel U, Bennemann U, Buerke M, Hattar K, Seeger W, Grimminger F, Sibelius U (2009) Staphylococcus aureus α-toxin and Escherichia coli hemolysin impair cardiac regional perfusion and contractile function by activating myocardial eicosanoid metabolism in isolated rat hearts. Crit Care Med 37(6):2025–2032. https://doi.org/10.1097/CCM.0b013e31819fff00

Grandi E, Morotti S, Ginsburg KS, Severi S, Bers DM (2010) Interplay of voltage and Ca-dependent inactivation of L-type Ca current. Prog Biophys Mol Biol 103(1):44–50. https://doi.org/10.1016/j.pbiomolbio.2010.02.001

Guatimosim S, Guatimosim C, Song LS (2011) Imaging calcium sparks in cardiac myocytes. Methods Mol Biol 689:205–214. https://doi.org/10.1007/978-1-60761-950-5_12

Guertl B, Noehammer C, Hoefler G (2000) Metabolic cardiomyopathies. Int J Exp Pathol 81(6):349–372 Retrieved from http://www.ncbi.nlm.nih.gov/pubmed/11298185

Guichard A, Nizet V, Bier E (2012) New insights into the biological effects of anthrax toxins: linking cellular to organismal responses. Microbes Infect 14(2):97–118. https://doi.org/10.1016/j.micinf.2011.08.016

Gurusamy N, Lekli I, Gorbunov NV, Gherghiceanu M, Popescu LM, Das DK (2009) Cardioprotection by adaptation to ischaemia augments autophagy in association with BAG-1 protein. J Cell Mol Med 13(2):373–387. https://doi.org/10.1111/j.1582-4934.2008.00495.x

Guvench O, Greene SN, Kamath G, Brady JW, Venable RM, Pastor RW, Mackerell AD (2008) Additive empirical force field for hexopyranose monosaccharides. J Comput Chem 29(15):2543–2564. https://doi.org/10.1002/jcc.21004

Hamm EE, Voth DE, Ballard JD (2006) Identification of Clostridium difficile toxin B cardiotoxicity using a zebrafish embryo model of intoxication. Proc Natl Acad Sci U S A 103(38):14176–14181. https://doi.org/10.1073/pnas.0604725103

Hanck DA, Sheets MF (1992) Time-dependent changes in kinetics of Na+ current in single canine cardiac Purkinje cells. Am J Physiol 262(4 Pt 2):H1197–H1207. https://doi.org/10.1152/ajpheart.1992.262.4.H1197

Hastings HM, Fenton FH, Evans SJ, Hotomaroglu O, Geetha J, Gittelson K, . . . Garfinkel A (2000) Alternans and the onset of ventricular fibrillation. Phys Rev E 62(3): 4043. https://doi.org/10.1103/physreve.62.4043.

Heath B, Terrar D (1996) Separation of the components of the delayed rectifier potassium current using selective blockers of IKr and IKs in guinea-pig isolated ventricular myocytes. Exp Physiol 81(4):587–603

Hedges PA, Hardy SJ (1996) Formation of disulfide bonded dimer of mutated heat-labile enterotoxin in vivo. FEBS Lett 381(1-2):53–56 Retrieved from http://www.ncbi.nlm.nih.gov/pubmed/8641438

Henrique C, Falcão MAP, De Araújo Pimenta L, Maleski ALA, Lima C, Mitsunari T, . . . Piazza RMF (2021) Heat-labile toxin from enterotoxigenic Escherichia coli causes systemic impairment in zebrafish model. Toxins (Basel) 13(6). https://doi.org/10.3390/toxins13060419

Higashi H, Omori A, Yamagata T (1992) Calmodulin, a ganglioside-binding protein. Binding of gangliosides to calmodulin in the presence of calcium. J Biol Chem 267(14):9831–9838 Retrieved from https://www.jbc.org/content/267/14/9831.full.pdf

Higginson EE, Sayeed MA, Pereira Dias J, Shetty V, Ballal M, Srivastava SK, . . . Mutreja A (2022) Microbiome profiling of enterotoxigenic Escherichia coli (ETEC) carriers highlights signature differences between symptomatic and asymptomatic individuals. MBio 13(3):e0015722. https://doi.org/10.1128/mbio.00157-22

Hilbush BS, Levine JM (1992) Modulation of a Ca2+ signaling pathway by GM1 ganglioside in PC12 cells. J Biol Chem 267(34):24789–24795 Retrieved from http://www.ncbi.nlm.nih.gov/pubmed/1447216

Hizo-Abes P, Clark WF, Sontrop JM, Young A, Huang A, Thiessen-Philbrook H, . . . Garg AX (2013) Cardiovascular disease after Escherichia coli O157:H7 gastroenteritis. CMAJ 185(1):E70-E77. https://doi.org/10.1503/cmaj.112161

Hoang-Trong MT, Ullah A, Lederer WJ, Jafri MS (2021) Cardiac alternans occurs through the synergy of voltage- and calcium-dependent mechanisms. Membranes (Basel) 11(10). https://doi.org/10.3390/membranes11100794

Hopenfeld B (2006) Mechanism for action potential alternans: the interplay between L-type calcium current and transient outward current. Heart Rhythm 3(3):345–352. https://doi.org/10.1016/j.hrthm.2005.11.016

Huang CL, Feng S, Hilgemann DW (1998) Direct activation of inward rectifier potassium channels by PIP2 and its stabilization by Gbetagamma. Nature 391(6669):803–806. https://doi.org/10.1038/35882

Huang XD, Wong TM (1989) Cholera toxin enhances ischemia-induced arrhythmias in the isolated rat heart--involvement of a guanine nucleotide binding protein (Gs). Life Sci 45(8):679–683. https://doi.org/10.1016/0024-3205(89)90085-4

Hünenberger PH (2005) Thermostat algorithms for molecular dynamics simulations. In: Holm C, Kremer K (eds) Advanced computer simulation. Advances in Polymer Science, vol. 173. Springer, Berlin, Heidelberg. https://doi.org/10.1007/b99427

Iacovache I, Bischofberger M, van der Goot FG (2010) Structure and assembly of pore-forming proteins. Curr Opin Struct Biol 20(2):241–246. https://doi.org/10.1016/j.sbi.2010.01.013

Israel CW (2014) Mechanisms of sudden cardiac death. Indian Heart J 66(Suppl 1(Suppl 1)):S10–S17. https://doi.org/10.1016/j.ihj.2014.01.005

Iwamoto R, Higashiyama S, Mitamura T, Taniguchi N, Klagsbrun M, Mekada E (1994) Heparin-binding EGF-like growth factor, which acts as the diphtheria toxin receptor, forms a complex with membrane protein DRAP27/CD9, which up-regulates functional receptors and diphtheria toxin sensitivity. EMBO J 13(10):2322–2330. https://doi.org/10.1002/j.1460-2075.1994.tb06516.x

Jeevaratnam K, Chadda KR, Huang CL, Camm AJ (2018) Cardiac potassium channels: physiological insights for targeted therapy. J Cardiovasc Pharmacol Ther 23(2):119–129. https://doi.org/10.1177/1074248417729880

Jiménez-Garduño AM, Mitkovski M, Alexopoulos IK, Sánchez A, Stühmer W, Pardo LA, Ortega A (2014) KV10.1 K(+)-channel plasma membrane discrete domain partitioning and its functional correlation in neurons. Biochim Biophys Acta 1838(3):921–931. https://doi.org/10.1016/j.bbamem.2013.11.007

Jin LM (2009) Rock 'n' Rho: regulation of ion channels. Am J Physiol Heart Circ Physiol 296(4):H908–H909. https://doi.org/10.1152/ajpheart.00185.2009

Jo S, Kim T, Iyer VG, Im W (2008) CHARMM-GUI: a web-based graphical user interface for CHARMM. J Comput Chem 29(11):1859–1865. https://doi.org/10.1002/jcc.20945

Jo SH, Lee SY (2010) Response of i(kr) and HERG currents to the antipsychotics tiapride and sulpiride. Korean J Physiol Pharmacol 14(5):305–310. https://doi.org/10.4196/kjpp.2010.14.5.305

Julien S, Bobowski M, Steenackers A, Le Bourhis X, Delannoy P (2013) How do gangliosides regulate RTKs signaling? Cells 2(4):751–767. https://doi.org/10.3390/cells2040751

Kaper JB, Nataro JP, Mobley HL (2004) Pathogenic Escherichia coli. Nat Rev Microbiol 2(2):123–140. https://doi.org/10.1038/nrmicro818

Kato Y, Masumiya H, Agata N, Tanaka H, Shigenobu K (1996) Developmental changes in action potential and membrane currents in fetal, neonatal and adult guinea-pig ventricular myocytes. J Mol Cell Cardiol 28(7):1515–1522. https://doi.org/10.1006/jmcc.1996.0141

Kilpatrick RD, McAllister CJ, Kovesdy CP, Derose SF, Kopple JD, Kalantar-Zadeh K (2007) Association between serum lipids and survival in hemodialysis patients and impact of race. J Am Soc Nephrol 18(1):293–303. https://doi.org/10.1681/asn.2006070795

Kim JY, Goldenring JR, DeLorenzo RJ, Yu RK (1986) Gangliosides inhibit phospholipid-sensitive Ca2+-dependent kinase phosphorylation of rat myelin basic proteins. J Neurosci Res 15(2):159–166. https://doi.org/10.1002/jnr.490150205

Kim R, Cingolani O, Wittstein I, McLean R, Han L, Cheng K, . . . Tereshchenko LG (2014) Mechanical alternans is associated with mortality in acute hospitalized heart failure: prospective mechanical alternans study (MAS). Circ Arrhythm Electrophysiol 7(2):259-266. https://doi.org/10.1161/circep.113.000958

Klauda JB, Venable RM, Freites JA, O'Connor JW, Tobias DJ, Mondragon-Ramirez C, . . . Pastor RW (2010) Update of the CHARMM all-atom additive force field for lipids: validation on six lipid types. J Phys Chem B 114(23):7830-7843. https://doi.org/10.1021/jp101759q

Konradt C, Frigimelica E, Nothelfer K, Puhar A, Salgado-Pabon W, di Bartolo V, . . . Phalipon A (2011) The Shigella flexneri type three secretion system effector IpgD inhibits T cell migration by manipulating host phosphoinositide metabolism. Cell Host Microbe 9(4):263-272. https://doi.org/10.1016/j.chom.2011.03.010

Kornyeyev D, Reyes M, Escobar AL (2010) Luminal Ca(2+) content regulates intracellular Ca(2+) release in subepicardial myocytes of intact beating mouse hearts: effect of exogenous buffers. Am J Physiol Heart Circ Physiol 298(6):H2138–H2153. https://doi.org/10.1152/ajpheart.00885.2009

Krause KH, Fivaz M, Monod A, van der Goot FG (1998) Aerolysin induces G-protein activation and Ca2+ release from intracellular stores in human granulocytes. J Biol Chem 273(29):18122–18129. https://doi.org/10.1074/jbc.273.29.18122

Kulkarni K, Merchant FM, Kassab MB, Sana F, Moazzami K, Sayadi O, . . . Armoundas AA (2019) Cardiac alternans: mechanisms and clinical utility in arrhythmia prevention. J Am Heart Assoc 8(21):e013750. https://doi.org/10.1161/JAHA.119.013750

L'Heureux M, Sternberg M, Brath L, Turlington J, Kashiouris MG (2020) Sepsis-induced cardiomyopathy: a comprehensive review. Curr Cardiol Rep 22(5):35. https://doi.org/10.1007/s11886-020-01277-2

Lai YM, Coombes S, Thul R (2020) Calcium buffers and L-type calcium channels as modulators of cardiac subcellular alternans. Commun Nonlinear Sci Numer Simul 85:105181. https://doi.org/10.1016/j.cnsns.2020.105181

Laohachai KN, Bahadi R, Hardo MB, Hardo PG, Kourie JI (2003) The role of bacterial and non-bacterial toxins in the induction of changes in membrane transport: implications for diarrhea. Toxicon 42(7):687–707. https://doi.org/10.1016/j.toxicon.2003.08.010

Laurita KR, Rosenbaum DS (2008) Cellular mechanisms of arrhythmogenic cardiac alternans. Prog Biophys Mol Biol 97(2-3):332–347. https://doi.org/10.1016/j.pbiomolbio.2008.02.014

Ledeen RW, Wu G (2002) Ganglioside function in calcium homeostasis and signaling. Neurochem Res 27(7-8):637–647 Retrieved from http://www.ncbi.nlm.nih.gov/pubmed/12374199

Ledeen RW, Wu G (2015) The multi-tasked life of GM1 ganglioside, a true factotum of nature. Trends Biochem Sci 40(7):407–418. https://doi.org/10.1016/j.tibs.2015.04.005

Lee J, Cheng X, Swails JM, Yeom MS, Eastman PK, Lemkul JA, . . . Im W (2016) CHARMM-GUI input generator for NAMD, GROMACS, AMBER, OpenMM, and CHARMM/OpenMM simulations using the CHARMM36 additive force field. J Chem Theory Comput 12(1):405-413. https://doi.org/10.1021/acs.jctc.5b00935

Lesieur C, Vécsey-Semjén B, Abrami L, Fivaz M, Gisou van der Goot F (1997) Membrane insertion: the strategies of toxins (review). Mol Membr Biol 14(2):45–64. https://doi.org/10.3109/09687689709068435

Lloyd KO, Furukawa K (1998) Biosynthesis and functions of gangliosides: recent advances. Glycoconj J 15(7):627–636 Retrieved from http://www.ncbi.nlm.nih.gov/pubmed/9881769

Lodovici M, Dolara P, Amerini S, Mantelli L, Ledda F, Bennardini F, . . . Dini G (1993) Effects of GM1 ganglioside on cardiac function following experimental hypoxia-reoxygenation. Eur J Pharmacol 243(3):255-263. Retrieved from http://www.ncbi.nlm.nih.gov/pubmed/8276078

Lopez JR, Jovanovic A, Terzic A (1995) Spontaneous calcium waves without contraction in cardiac myocytes. Biochem Biophys Res Commun 214(3):781–787. https://doi.org/10.1006/bbrc.1995.2354

Los FC, Randis TM, Aroian RV, Ratner AJ (2013) Role of pore-forming toxins in bacterial infectious diseases. Microbiol Mol Biol Rev 77(2):173–207. https://doi.org/10.1128/mmbr.00052-12

Lozano MM, Liu Z, Sunnick E, Janshoff A, Kumar K, Boxer SG (2013) Colocalization of the ganglioside G(M1) and cholesterol detected by secondary ion mass spectrometry. J Am Chem Soc 135(15):5620–5630. https://doi.org/10.1021/ja310831m

Lu HK, Fern RJ, Nee JJ, Barrett PQ (1994) Ca(2+)-dependent activation of T-type Ca2+ channels by calmodulin-dependent protein kinase II. Am J Physiol 267(1 Pt 2):F183–F189 Retrieved from http://www.ncbi.nlm.nih.gov/pubmed/8048559

Lunghi G, Fazzari M, Di Biase E, Mauri L, Sonnino S, Chiricozzi E (2020) Modulation of calcium signaling depends on the oligosaccharide of GM1 in Neuro2a mouse neuroblastoma cells. Glycoconj J 37(6):713–727. https://doi.org/10.1007/s10719-020-09963-7

Maguy A, Hebert TE, Nattel S (2006) Involvement of lipid rafts and caveolae in cardiac ion channel function. Cardiovasc Res 69(4):798–807. https://doi.org/10.1016/j.cardiores.2005.11.013

Mahajan A, Sato D, Shiferaw Y, Baher A, Xie LH, Peralta R, . . . Weiss JN (2008) Modifying L-type calcium current kinetics: consequences for cardiac excitation and arrhythmia dynamics. Biophys J 94(2):411-423. https://doi.org/10.1529/biophysj.106.98590

Mahfoud R, Manis A, Binnington B, Ackerley C, Lingwood CA (2010) A major fraction of glycosphingolipids in model and cellular cholesterol-containing membranes is undetectable by their binding proteins. J Biol Chem 285(46):36049–36059. https://doi.org/10.1074/jbc.M110.110189

Maltsev VA, Undrovinas AI (1997) Cytoskeleton modulates coupling between availability and activation of cardiac sodium channel. Am J Physiol 273(4):H1832–H1840. https://doi.org/10.1152/ajpheart.1997.273.4.H1832

Mangold, K. E., Brumback, B. D., Angsutararux, P., Voelker, T. L., Zhu, W., Kang, P. W., . . . Silva, J. R. (2017). Mechanisms and models of cardiac sodium channel inactivation. Channels (Austin), 11(6), 517-533. https://doi.org/10.1080/19336950.2017.1369637

Marbán E (1999) Heart failure: the electrophysiologic connection. J Cardiovasc Electrophysiol 10(10):1425–1428. https://doi.org/10.1111/j.1540-8167.1999.tb00199.x

Marengo FD, Wang SY, Wang B, Langer GA (1998) Dependence of cardiac cell Ca2+ permeability on sialic acid-containing sarcolemmal gangliosides. J Mol Cell Cardiol 30(1):127–137. https://doi.org/10.1006/jmcc.1997.0579

Marks AR (1997) Intracellular calcium-release channels: regulators of cell life and death. Am J Physiol 272(2 Pt 2):H597–H605 Retrieved from http://www.ncbi.nlm.nih.gov/pubmed/9124414

Masignani V, Pizza M, Rappuoli R (2006) Bacterial toxins. In: Dworkin M, Falkow S, Rosenberg E, Schleifer KH, Stackebrandt E (eds) The Prokaryotes. Springer, New York, NY. https://doi.org/10.1007/0-387-30742-7_28

Maury P, Extramiana F, Giustetto C, Cardin C, Rollin A, Duparc A, . . . Marangoni D (2012) Microvolt T-wave alternans in short QT syndrome. Pacing Clin Electrophysiol 35(12):1413-1419. https://doi.org/10.1111/j.1540-8159.2012.03491.x

Mergler S, Dannowski H, Bednarz J, Engelmann K, Hartmann C, Pleyer U (2003) Calcium influx induced by activation of receptor tyrosine kinases in SV40-transfected human corneal endothelial cells. Exp Eye Res 77(4):485–495. https://doi.org/10.1016/s0014-4835(03)00154-4

Merritt EA, Kuhn P, Sarfaty S, Erbe JL, Holmes RK, Hol WGJ (1998) The 1.25 Å resolution refinement of the cholera toxin B-pentamer: evidence of peptide backbone strain at the receptor-binding site11Edited by I. A. Wilson. J Mol Biol 282(5):1043–1059. https://doi.org/10.1006/jmbi.1998.2076

Merritt EA, Sarfaty S, van den Akker F, L'Hoir C, Martial JA, Hol WG (1994) Crystal structure of cholera toxin B-pentamer bound to receptor GM1 pentasaccharide. Protein Sci 3(2):166–175. https://doi.org/10.1002/pro.5560030202

Milani D, Minozzi MC, Petrelli L, Guidolin D, Skaper SD, Spoerri PE (1992) Interaction of ganglioside GM1 with the B subunit of cholera toxin modulates intracellular free calcium in sensory neurons. J Neurosci Res 33(3):466–475. https://doi.org/10.1002/jnr.490330313

Miller WC, Palmer WK, Arnall DA, Oscai LB (1987) Effect of cholera toxin on triacylglycerol lipase activity and triacylglycerol content of rat heart. Can J Physiol Pharmacol 65(1):60–63. https://doi.org/10.1139/y87-011

Millet J, Aguilar-Sanchez Y, Kornyeyev D, Bazmi M, Fainstein D, Copello JA, Escobar AL (2021) Thermal modulation of epicardial Ca2+ dynamics uncovers molecular mechanisms of Ca2+ alternans. J Gen Physiol 153(2). https://doi.org/10.1085/jgp.202012568

Minke WE, Roach C, Hol WG, Verlinde CLJB (1999) Structure-based exploration of the ganglioside GM1 binding sites of Escherichia coli heat-labile enterotoxin and cholera toxin for the discovery of receptor antagonists. Biochemistry 38(18):5684–5692. https://doi.org/10.1021/bi982649a

Mitchell DD, Pickens JC, Korotkov K, Fan E, Hol WGJ (2004) 3,5-Substituted phenyl galactosides as leads in designing effective cholera toxin antagonists. Bioorg Med Chem 12(5):907–920. https://doi.org/10.1016/j.bmc.2003.12.019

Mitra R, Morad M (1985) A uniform enzymatic method for dissociation of myocytes from hearts and stomachs of vertebrates. Am J Physiol 249(5 Pt 2):H1056–H1060 Retrieved from http://www.ncbi.nlm.nih.gov/pubmed/2998207

Monticelli J, Di Bella S, Di Masi A, Zennaro C, Tonon F, Luzzati R (2018) Septic cardiomyopathy and bacterial exotoxins. Crit Care Med 46(9):e965–e966. https://doi.org/10.1097/ccm.0000000000003217

Montpetit ML, Stocker PJ, Schwetz TA, Harper JM, Norring SA, Schaffer L, . . . Bennett ES (2009) Regulated and aberrant glycosylation modulate cardiac electrical signaling. Proc Natl Acad Sci USA 106(38):16517-16522. https://doi.org/10.1073/pnas.0905414106

Morris JA, Harrison L, Brodison A, Lauder R (2009) Sudden infant death syndrome and cardiac arrhythmias. Future Cardiol 5(2):201–207. https://doi.org/10.2217/14796678.5.2.201

Mudrak B, Kuehn MJ (2010) Heat-labile enterotoxin: beyond G(m1) binding. Toxins (Basel) 2(6):1445–1470. https://doi.org/10.3390/toxins2061445

Murrell WG, Stewart BJ, O'Neill C, Siarakas S, Kariks S (1993) Enterotoxigenic bacteria in the sudden infant death syndrome. J Med Microbiol 39(2):114–127. https://doi.org/10.1099/00222615-39-2-114

Musher DM, Musher BL (2004) Contagious acute gastrointestinal infections. N Engl J Med 351(23):2417–2427. https://doi.org/10.1056/NEJMra041837

Nicoli ER, Annunziata I, d'Azzo A, Platt FM, Tifft CJ, Stepien KM (2021) GM1 gangliosidosis-a mini-review. Front Genet 12:734878. https://doi.org/10.3389/fgene.2021.734878

Nie HG, Hao LY, Xu JJ, Minobe E, Kameyama A, Kameyama M (2007) Distinct roles of CaM and Ca(2+)/CaM -dependent protein kinase II in Ca(2+) -dependent facilitation and inactivation of cardiac L-type Ca(2+) channels. J Physiol Sci 57(3):167–173. https://doi.org/10.2170/physiolsci.RP000507

Olson RD, Stevens DL, Melish ME (1989) Direct effects of purified staphylococcal toxic shock syndrome toxin 1 on myocardial function of isolated rabbit atria. Rev Infect Dis 11(Suppl 1):S313–S315. https://doi.org/10.1093/clinids/11.supplement_1.s313

Orlandi PA, Fishman PH (1998) Filipin-dependent inhibition of cholera toxin: evidence for toxin internalization and activation through caveolae-like domains. J Cell Biol 141(4):905–915. https://doi.org/10.1083/jcb.141.4.905

Ostolaza H, González-Bullón D, Uribe KB, Martín C, Amuategi J, Fernandez-Martínez X (2019) Membrane permeabilization by pore-forming RTX toxins: what kind of lesions do these toxins form? Toxins (Basel) 11(6). https://doi.org/10.3390/toxins11060354

Pani B, Singh BB (2009) Lipid rafts/caveolae as microdomains of calcium signaling. Cell Calcium 45(6):625–633. https://doi.org/10.1016/j.ceca.2009.02.009

Panicker GK, Manohar D, Karnad DR, Salvi V, Kothari S, Lokhandwala Y (2012) Early repolarization and short QT interval in healthy subjects. Heart Rhythm 9(8):1265–1271. https://doi.org/10.1016/j.hrthm.2012.03.046

Pásek M, Šimurda J, Orchard CH, Christé G (2008) A model of the guinea-pig ventricular cardiac myocyte incorporating a transverse–axial tubular system. Prog Biophys Mol Biol 96(1):258–280. https://doi.org/10.1016/j.pbiomolbio.2007.07.022

Patry RT, Stahl M, Perez-Munoz ME, Nothaft H, Wenzel CQ, Sacher JC, . . . Szymanski CM (2019) Bacterial AB 5 toxins inhibit the growth of gut bacteria by targeting ganglioside-like glycoconjugates. Nat Commun 10(1):1-13. https://doi.org/10.1038/s41467-019-09362-z.

Pei B, Liu Z-P, Chen J-W (2002) Ganglioside GM1 biphasically regulates the activity of protein kinase C by the effects on the structure of the lipid bilayer. Chem Phys Lipids 114(2):131–138. https://doi.org/10.1016/S0009-3084(01)00193-1

Peterson BZ, DeMaria CD, Adelman JP, Yue DT (1999) Calmodulin is the Ca2+ sensor for Ca2+ -dependent inactivation of L-type calcium channels. Neuron 22(3):549–558. https://doi.org/10.1016/s0896-6273(00)80709-6

Ponce-Balbuena D, Guerrero-Serna G, Valdivia CR, Caballero R, Diez-Guerra FJ, Jiménez-Vázquez EN, . . . Jalife J (2018) Cardiac Kir2.1 and Na(V)1.5 channels traffic together to the sarcolemma to control excitability. Circ Res 122(11):1501-1516. https://doi.org/10.1161/circresaha.117.311872

Popoff MR, Poulain B (2010) Bacterial toxins and the nervous system: neurotoxins and multipotential toxins interacting with neuronal cells. Toxins (Basel) 2(4):683–737. https://doi.org/10.3390/toxins2040683

Posse de Chaves E, Sipione S (2010) Sphingolipids and gangliosides of the nervous system in membrane function and dysfunction. FEBS Lett 584(9):1748–1759. https://doi.org/10.1016/j.febslet.2009.12.010

Puglisi JL, Bers DM (2001) LabHEART: An interactive computer model of rabbit ventricular myocyte ion channels and Ca

transport. Am J Physiol Cell Physiol 281(6):C2049–C2060. https://doi.org/10.1152/ajpcell.2001.281.6.C2049
Qiao GF, Cheng ZF, Huo R, Sui XH, Lu YJ, Li BY (2008) GM1 ganglioside contributes to retain the neuronal conduction and neuronal excitability in visceral and baroreceptor afferents. J Neurochem 106(4):1637–1645. https://doi.org/10.1111/j.1471-4159.2008.05515.x
Qu Z, Weiss JN (2023) Cardiac alternans: from bedside to bench and back. Circ Res 132(1):127–149. https://doi.org/10.1161/CIRCRESAHA.122.321668
Rahman MM, Islam F, Or-Rashid MH, Mamun AA, Rahaman MS, Islam MM, . . . Cavalu S (2022) The gut microbiota (microbiome) in cardiovascular disease and its therapeutic regulation. Front Cell Infect Microbiol 12:903570. https://doi.org/10.3389/fcimb.2022.903570
Ravichandra B, Joshi PG (1999) Regulation of transmembrane signaling by ganglioside GM1: interaction of anti-GM1 with Neuro2a cells. J Neurochem 73(2):557–567 Retrieved from http://www.ncbi.nlm.nih.gov/pubmed/10428051
Robert F, Marjana G, Milka V (2012) Cardiovascular pathophysiology produced by natural toxins and their possible therapeutic implications. In: Manuela F (ed) Cardiotoxicity of oncologic treatments (pp Ch 1). IntechOpen, Rijeka. https://doi.org/10.5772/35079
Rondelli V, Fragneto G, Motta S, Del Favero E, Brocca P, Sonnino S, Cantù L (2012) Ganglioside GM1 forces the redistribution of cholesterol in a biomimetic membrane. Biochim Biophys Acta 1818(11):2860–2867. https://doi.org/10.1016/j.bbamem.2012.07.010
Rosenbaum DS, Jackson LE, Smith JM, Garan H, Ruskin JN, Cohen RJ (1994) Electrical alternans and vulnerability to ventricular arrhythmias. N Engl J Med 330(4):235–241. https://doi.org/10.1056/NEJM199401273300402
Rubenstein DS, Lipsius SL (1995) Premature beats elicit a phase reversal of mechanoelectrical alternans in cat ventricular myocytes. A possible mechanism for reentrant arrhythmias. Circulation 91(1):201–214. https://doi.org/10.1161/01.cir.91.1.201
Ryckeart J-P, Ciccoti G, Berendsen HCP (1977) Numerical integration of the Cartesian equations of motion of a system with constraints: Molecular dynamics of n-alkanes. J Comput Phys 23:327–341. https://doi.org/10.1016/0021-9991(77)90098-5
Sanguinetti MC, Jurkiewicz NK (1990) Two components of cardiac delayed rectifier K+ current: differential sensitivity to block by class III antiarrhythmic agents. J Gen Physiol 96(1):195–215. https://doi.org/10.1085/jgp.96.1.195
Sarusi A, Rárosi F, Szűcs M, Csík N, Farkas AS, Papp JG, . . . Farkas A (2014) Absolute beat-to-beat variability and instability parameters of ECG intervals: biomarkers for predicting ischaemia-induced ventricular fibrillation. Br J Pharmacol 171(7):1772-1782. https://doi.org/10.1111/bph.12579
Schnaar RL (2010) Brain gangliosides in axon-myelin stability and axon regeneration. FEBS Lett 584(9):1741–1747. https://doi.org/10.1016/j.febslet.2009.10.011
Shaughnessy LM, Hoppe AD, Christensen KA, Swanson JA (2006) Membrane perforations inhibit lysosome fusion by altering pH and calcium in Listeria monocytogenes vacuoles. Cell Microbiol 8(5):781–792. https://doi.org/10.1111/j.1462-5822.2005.00665.x
Short B (2021) Understanding Ca2+ alternans. J Gen Physiol 153(2). https://doi.org/10.1085/jgp.202112862
Siarakas S, Brown AJ, Murrell WG (1999) Immunological evidence for a bacterial toxin aetiology in sudden infant death syndrome. FEMS Immunol Med Microbiol 25(1-2):37–50 Retrieved from http://www.ncbi.nlm.nih.gov/pubmed/10443490
Silversides JA, Lappin E, Ferguson AJ (2010) Staphylococcal toxic shock syndrome: mechanisms and management. Curr Infect Dis Rep 12(5):392–400. https://doi.org/10.1007/s11908-010-0119-y
Simons K, Toomre D (2000) Lipid rafts and signal transduction. Nat Rev Mol Cell Biol 1(1):31–39. https://doi.org/10.1038/35036052
Singh S, Gupta N, Saple P (2020) Diphtheritic myocarditis: a case series and review of literature. J Family Med Prim Care 9(11):5769–5771. https://doi.org/10.4103/jfmpc.jfmpc_1396_20
Sixma TK, Kalk KH, van Zanten BA, Dauter Z, Kingma J, Witholt B, Hol WG (1993) Refined structure of Escherichia coli heat-labile enterotoxin, a close relative of cholera toxin. J Mol Biol 230(3):890–918. https://doi.org/10.1006/jmbi.1993.1209
Skardal PS, Restrepo JG (2014) Coexisting chaotic and multi-periodic dynamics in a model of cardiac alternans. Chaos 24(4):043126. https://doi.org/10.1063/1.4901728
Slomiany BL, Liu J, Fekete Z, Yao P, Slomiany A (1992) Modulation of dihydropyridine-sensitive gastric mucosal calcium channels by GM1-ganglioside. Int J Biochem 24(8):1289–1294 Retrieved from http://www.ncbi.nlm.nih.gov/pubmed/1322845
Smith DC, Lord JM, Roberts LM, Johannes L (2004) Glycosphingolipids as toxin receptors. Semin Cell Dev Biol 15(4):397–408. https://doi.org/10.1016/j.semcdb.2004.03.005
Soderblom T, Laestadius A, Oxhamre C, Aperia A, Richter-Dahlfors A (2002) Toxin-induced calcium oscillations: a novel strategy to affect gene regulation in target cells. Int J Med Microbiol 291(6-7):511–515 Retrieved from http://www.ncbi.nlm.nih.gov/pubmed/11890551
Spangler BD (1992) Structure and function of cholera toxin and the related Escherichia coli heat-labile enterotoxin. Microbiol Rev 56(4):622–647 Retrieved from http://www.ncbi.nlm.nih.gov/pubmed/1480112
Spiegel S, Panagiotopoulos C (1988) Mitogenesis of 3T3 fibroblasts induced by endogenous ganglioside is not mediated by cAMP, protein kinase C, or phosphoinositides turnover. Exp Cell Res 177(2):414–427 Retrieved from http://www.ncbi.nlm.nih.gov/pubmed/2839353
Staali L, Monteil H, Colin DA (1998) The staphylococcal pore-forming leukotoxins open Ca2+ channels in the membrane of human polymorphonuclear neutrophils. J Membr Biol 162(3):209–216. https://doi.org/10.1007/s002329900358
Suffredini DA, Sampath-Kumar H, Li Y, Ohanjanian L, Remy KE, Cui X, Eichacker PQ (2015) Does Bacillus anthracis lethal toxin directly depress myocardial function? A review of clinical cases and preclinical studies. Toxins (Basel) 7(12):5417–5434. https://doi.org/10.3390/toxins7124891
Tanaka H, Habuchi Y, Lu L-L, Furukawa T, Morikawa J, Yoshimura M (1994) Modulation of sodium current by lactate in guinea pig ventricular myocytes. Cardiovasc Res 28(10):1507–1512. https://doi.org/10.1093/cvr/28.10.1507
Tarvainen MP, Niskanen J-P, Lipponen JA, Ranta-Aho PO, Karjalainen PA (2014) Kubios HRV–heart rate variability analysis software. Comput Methods Programs Biomed 113(1):210–220. https://doi.org/10.1016/j.cmpb.2013.07.024
Thiagarajah JR, Verkman AS (2005) New drug targets for cholera therapy. Trends Pharmacol Sci 26(4):172–175. https://doi.org/10.1016/j.tips.2005.02.003
Tran Van Nhieu G, Kai Liu B, Zhang J, Pierre F, Prigent S, Sansonetti P, . . . Combettes L (2013) Actin-based confinement of calcium responses during Shigella invasion. Nat Commun 4:1567. https://doi.org/10.1038/ncomms2561
TranVan Nhieu G, Clair C, Grompone G, Sansonetti P (2004) Calcium signalling during cell interactions with bacterial pathogens. Biol Cell 96(1):93–101. https://doi.org/10.1016/j.biolcel.2003.10.006
Tse G, Chan YWF, Keung W, Yan BP (2017) Electrophysiological mechanisms of long and short QT syndromes. IJC Heart Vasc 14:8–13. https://doi.org/10.1016/j.ijcha.2016.11.006
Tveito A, Lines GT, Edwards AG, Maleckar MM, Michailova A, Hake J, McCulloch A (2012) Slow calcium-depolarization-calcium waves may initiate fast local depolarization waves in ventricular tissue. Prog Biophys Mol Biol 110(2-3):295–304. https://doi.org/10.1016/j.pbiomolbio.2012.07.005

Tzimas C, Johnson DM, Santiago DJ, Vafiadaki E, Arvanitis DA, Davos CH, . . . Sanoudou D (2017) Impaired calcium homeostasis is associated with sudden cardiac death and arrhythmias in a genetic equivalent mouse model of the human HRC-Ser96Ala variant. Cardiovasc Res 113(11):1403-1417. https://doi.org/10.1093/cvr/cvx113

Verrier RL, Nearing BD (1994) Electrophysiologic basis for T wave alternans as an index of vulnerability to ventricular fibrillation. J Cardiovasc Electrophysiol 5(5):445–461 Retrieved from http://www.ncbi.nlm.nih.gov/pubmed/8055149

Virk HU, Inayat F (2016) Clostridium difficile infection and takotsubo cardiomyopathy: is there a relation? N Am J Med Sci 8(7):316–319. https://doi.org/10.4103/1947-2714.187156

Wagner S, Maier LS, Bers DM (2015) Role of sodium and calcium dysregulation in tachyarrhythmias in sudden cardiac death. Circ Res 116(12):1956–1970. https://doi.org/10.1161/circresaha.116.304678

Walker ML, Rosenbaum DS (2005) Cellular alternans as mechanism of cardiac arrhythmogenesis. Heart Rhythm 2(12):1383–1386. https://doi.org/10.1016/j.hrthm.2005.09.009

Wanford JJ, Odendall C (2023) Ca(2+)-calmodulin signalling at the host-pathogen interface. Curr Opin Microbiol 72:102267. https://doi.org/10.1016/j.mib.2023.102267

Wang G, Alhamdi Y, Toh C-H (2017) 143 The roles and mechanisms of pore-forming toxins in cardiac injury. Heart 103(Suppl 5):A107–A107. https://doi.org/10.1136/heartjnl-2017-311726.142

Wang HW, Yang ZF, Zhang Y, Yang JM, Liu YM, Li CZ (2009) Beta-receptor activation increases sodium current in guinea pig heart. Acta Pharmacol Sin 30(8):1115–1122. https://doi.org/10.1038/aps.2009.96

Wang SQ, Wei C, Zhao G, Brochet DX, Shen J, Song LS, . . . Cheng H (2004) Imaging microdomain Ca2+ in muscle cells. Circ Res 94(8):1011-1022. https://doi.org/10.1161/01.RES.0000125883.68447.A1

Wasserstrom JA, Vites AM (1999) Activation of contraction in cat ventricular myocytes: effects of low Cd(2+) concentration and temperature. Am J Physiol 277(2):H488–H498. https://doi.org/10.1152/ajpheart.1999.277.2.H488

Wei, J., Yao, J., Belke, D., Guo, W., Zhong, X., Sun, B., . . . Chen, S. R. W. (2021). Ca(2+)-CaM dependent inactivation of RyR2 underlies Ca(2+) alternans in intact heart. Circ Res, 128(4), e63-e83. https://doi.org/10.1161/circresaha.120.318429

Weiss JN, Karma A, Shiferaw Y, Chen PS, Garfinkel A, Qu Z (2006) From pulsus to pulseless: the saga of cardiac alternans. Circ Res 98(10):1244–1253. https://doi.org/10.1161/01.RES.0000224540.97431.f0

Wernick NL, Chinnapen DJ, Cho JA, Lencer WI (2010) Cholera toxin: an intracellular journey into the cytosol by way of the endoplasmic reticulum. Toxins (Basel) 2(3):310–325. https://doi.org/10.3390/toxins2030310

Wilson LD, Jeyaraj D, Wan X, Hoeker GS, Said TH, Gittinger M, . . . Rosenbaum DS (2009) Heart failure enhances susceptibility to arrhythmogenic cardiac alternans. Heart Rhythm 6(2):251-259. https://doi.org/10.1016/j.hrthm.2008.11.008

Wilson LD, Rosenbaum DS (2007) Mechanisms of arrythmogenic cardiac alternans. Europace 9(Suppl 6):vi77-82. https://doi.org/10.1093/europace/eum210

Wilson LD, Wan X, Rosenbaum DS (2006) Cellular alternans: a mechanism linking calcium cycling proteins to cardiac arrhythmogenesis. Ann N Y Acad Sci 1080:216–234. https://doi.org/10.1196/annals.1380.018

Witkowski M, Weeks TL, Hazen SL (2020) Gut microbiota and cardiovascular disease. Circ Res 127(4):553–570. https://doi.org/10.1161/CIRCRESAHA.120.316242

Wolf AA, Jobling MG, Wimer-Mackin S, Ferguson-Maltzman M, Madara JL, Holmes RK, Lencer WI (1998) Ganglioside structure dictates signal transduction by cholera toxin and association with caveolae-like membrane domains in polarized epithelia. J Cell Biol 141(4):917–927. https://doi.org/10.1083/jcb.141.4.917

Wu CC, Su MJ, Chi JF, Chen WJ, Hsu HC, Lee YT (1995) The effect of hypercholesterolemia on the sodium inward currents in cardiac myocyte. J Mol Cell Cardiol 27(6):1263–1269. https://doi.org/10.1016/s0022-2828(05)82388-0

Wu G, Lu ZH, Nakamura K, Spray DC, Ledeen RW (1996) Trophic effect of cholera toxin B subunit in cultured cerebellar granule neurons: modulation of intracellular calcium by GM1 ganglioside. J Neurosci Res 44(3):243–254. https://doi.org/10.1002/(SICI)1097-4547(19960501)44:3<243::AID-JNR5>3.0.CO;2-G

Xu J, Zhang S, Zhao S, Hu L (2020) Identification and synthesis of an efficient multivalent E. coli heat labile toxin inhibitor (__) a dynamic combinatorial chemistry approach. Bioorg Med Chem 28(9):115436. https://doi.org/10.1016/j.bmc.2020.115436

Yamashita T, Yoshida N, Emoto T, Saito Y, Hirata KI (2021) Two gut microbiota-derived toxins are closely associated with cardiovascular diseases: a review. Toxins (Basel) 13(5). https://doi.org/10.3390/toxins13050297

Yesilbas O, Yozgat CY, Akinci N, Talebazadeh F, Jafarov U, Guney AZ, . . . Yozgat Y (2020) Sudden cardiac arrest and malignant ventricular tachycardia in an 8-year-old pediatric patient who has hemolytic uremic syndrome associated with shiga toxin-producing Escherichia coli. J Pediatr Intensive Care 9(4):290-294. https://doi.org/10.1055/s-0040-1708553

You T, Luo C, Zhang K, Zhang H (2021) Electrophysiological mechanisms underlying T-wave alternans and their role in arrhythmogenesis. Front Physiol 12(235). https://doi.org/10.3389/fphys.2021.614946

Zareba W, Cygankiewicz I (2008) Long QT syndrome and short QT syndrome. Prog Cardiovasc Dis 51(3):264–278. https://doi.org/10.1016/j.pcad.2008.10.006

Zeller CB, Marchase RB (1992) Gangliosides as modulators of cell function. Am J Physiol 262(6 Pt 1):C1341–C1355 Retrieved from http://www.ncbi.nlm.nih.gov/pubmed/1616002

Zhao Y, Hu HY, Sun DR, Feng R, Sun XF, Guo F, Hao LY (2014) Dynamic alterations in the CaV1.2/CaM/CaMKII signaling pathway in the left ventricular myocardium of ischemic rat hearts. DNA Cell Biol 33(5):282–290. https://doi.org/10.1089/dna.2013.2231

Zhong Q, Roumeliotis TI, Kozik Z, Cepeda-Molero M, Fernández L, Shenoy AR, . . . Choudhary JS (2020)Clustering of Tir during enteropathogenic E. coli infection triggers calcium influx-dependent pyroptosis in intestinal epithelial cells. PLoS Biol, 18(12), e3000986. https://doi.org/10.1371/journal.pbio.3000986

Zhu C, Setty P, Boedeker EC (2017) Development of live attenuated bacterial vaccines targeting Escherichia coli heat-labile and heat-stable enterotoxins. Vet Microbiol 202:72–78. https://doi.org/10.1016/j.vetmic.2017.04.010

Zivich PN, Grabenstein JD, Becker-Dreps SI, Weber DJ (2018) Streptococcus pneumoniae outbreaks and implications for transmission and control: a systematic review. Pneumonia (Nathan) 10:11. https://doi.org/10.1186/s41479-018-0055-4